



ARL-TR-7275 • APR 2015



US Army Research Laboratory

# **Design of Experiment Approach to Hydrogen Re-embrittlement Evaluation WP-2152**

**by Scott M Grendahl, Hoang Nguyen, Franklin Kellogg, Shuying  
Zhu, and Stephen Jones**

Approved for public release; distribution is unlimited.

## **NOTICES**

### **Disclaimers**

The findings in this report are not to be construed as an official Department of the Army position unless so designated by other authorized documents.

Citation of manufacturer's or trade names does not constitute an official endorsement or approval of the use thereof.

Destroy this report when it is no longer needed. Do not return it to the originator.



# **Design of Experiment Approach to Hydrogen Re-embrittlement Evaluation WP-2152**

**Scott M Grendahl**

*Weapons and Materials Research Directorate, ARL*

**Hoang Nguyen and Franklin Kellogg**

*Bowhead Science and Technology, LLC*

**Shuying Zhu and Stephen Jones**

*The Boeing Company*

REPORT DOCUMENTATION PAGE				Form Approved OMB No. 0704-0188	
<p>Public reporting burden for this collection of information is estimated to average 1 hour per response, including the time for reviewing instructions, searching existing data sources, gathering and maintaining the data needed, and completing and reviewing the collection information. Send comments regarding this burden estimate or any other aspect of this collection of information, including suggestions for reducing the burden, to Department of Defense, Washington Headquarters Services, Directorate for Information Operations and Reports (0704-0188), 1215 Jefferson Davis Highway, Suite 1204, Arlington, VA 22202-4302. Respondents should be aware that notwithstanding any other provision of law, no person shall be subject to any penalty for failing to comply with a collection of information if it does not display a currently valid OMB control number.</p> <p><b>PLEASE DO NOT RETURN YOUR FORM TO THE ABOVE ADDRESS.</b></p>					
1. REPORT DATE (DD-MM-YYYY) April 2015		2. REPORT TYPE Final		3. DATES COVERED (From - To) January 2011–August 2014	
4. TITLE AND SUBTITLE Design of Experiment Approach to Hydrogen Re-embrittlement Evaluation WP-2152				5a. CONTRACT NUMBER	
				5b. GRANT NUMBER	
				5c. PROGRAM ELEMENT NUMBER	
6. AUTHOR(S) Scott M Grendahl, Hoang Nguyen, Franklin Kellogg, Shuying Zhu, and Stephen Jones				5d. PROJECT NUMBER W74RDV20769717	
				5e. TASK NUMBER	
				5f. WORK UNIT NUMBER	
7. PERFORMING ORGANIZATION NAME(S) AND ADDRESS(ES) US Army Research Laboratory ATTN: RDRL-WMM-F Aberdeen Proving Ground, MD 21005-5069				8. PERFORMING ORGANIZATION REPORT NUMBER  ARL-TR-7275	
9. SPONSORING/MONITORING AGENCY NAME(S) AND ADDRESS(ES) Strategic Environmental Research and Development Program (SERDP)/ Environmental Security Technology Certification Program (ESTCP) 4800 Mark Center Drive, Suite 17D08 Alexandria, VA 22350-3605				10. SPONSOR/MONITOR'S ACRONYM(S)	
				11. SPONSOR/MONITOR'S REPORT NUMBER(S)	
12. DISTRIBUTION/AVAILABILITY STATEMENT Approved for public release; distribution is unlimited.					
13. SUPPLEMENTARY NOTES					
14. ABSTRACT A 3-phase design-of-experiment approach was used to investigate hydrogen re-embrittlement effects of common aviation maintenance chemicals and coatings. Both material and geometry were examined to uncover the best constraints for a novel method. While traditional testing uses a pass/fail approach, the developed method employed load monitoring cells over a range of material strength, hydrogen-emitting environment, and applied load. This method allowed prospective solvent replacement chemicals and cadmium replacement coatings to be finely delineated in terms of performance and formed the basis of a tool for predicting time to failure under any combination of parameters. In the aviation community, heavy restriction on using alternative chemicals and coatings could therefore be eased, and applications could be expanded for using high-strength steel.					
15. SUBJECT TERMS hydrogen, embrittlement, 4340 steel, aqueous cleaning, cadmium plating alternatives					
16. SECURITY CLASSIFICATION OF:			17. LIMITATION OF ABSTRACT  UU	18. NUMBER OF PAGES  64	19a. NAME OF RESPONSIBLE PERSON Scott M Grendahl
a. REPORT Unclassified	b. ABSTRACT Unclassified	c. THIS PAGE Unclassified			19b. TELEPHONE NUMBER (Include area code) 410-306-0819

## Contents

---

<b>List of Figures</b>	<b>v</b>
<b>List of Tables</b>	<b>vii</b>
<b>Acknowledgments</b>	<b>viii</b>
<b>1. Introduction and Background</b>	<b>1</b>
<b>2. Phase 1</b>	<b>4</b>
2.1 Introduction	4
2.2 Objective	4
2.3 Materials	4
2.3.1 Heat Treating	5
2.3.2 Cadmium Plating	6
2.4 Experimental Procedures	8
2.4.1 Design of Experiment	8
2.4.2 Specimens, Environment, and Loading	10
2.5 Results	14
2.6 Discussion	20
2.7 Conclusions	22
<b>3. Phase 2</b>	<b>22</b>
3.1 Introduction	22
3.2 Objective	23
3.3 Materials	23
3.3.1 Heat Treating	24
3.3.2 Maintenance Chemicals	24
3.4 Experimental Procedures	26
3.4.1 Design of Experiment	26
3.4.2 Specimens, Environment, and Loading	28
3.5 Results	29

3.6 Discussion	35
3.7 Conclusions	36
<b>4. Phase 3</b>	<b>36</b>
4.1 Introduction	36
4.2 Objective	37
4.3 Materials	37
4.3.1 Heat Treating	37
4.3.2 Coatings	38
4.3.3 Immersion Chemical	39
4.4 Experimental Procedures	39
4.4.1 Design of Experiment	39
4.2.2 Specimens, Environment, and Loading	42
4.5 Results	43
4.6 Discussion	49
4.7 Conclusions	50
<b>5. References</b>	<b>52</b>
<b>List of Symbols, Abbreviations, and Acronyms</b>	<b>53</b>
<b>Distribution List</b>	<b>54</b>

## List of Figures

---

Fig. 1	ASTM-F519 specimen geometries .....	5
Fig. 2	Masking/plating of the 5 specimen geometries .....	7
Fig. 3	Cadmium-plated experimental specimens 1a.1, 1a.2, 1c, 1d, and 1e (top to bottom) .....	11
Fig. 4	Geometry 1a.1 and 1a.2 in situ environmental setup: A) empty container, B) sample in the cup, C) sample loaded onto the mechanical test frame, and D) sample being tested in solution .....	12
Fig. 5	Geometry 1c in situ environmental setup: A) loaded, B) loaded and masked, and C) being tested in solution.....	12
Fig. 6	Geometry 1d in situ environmental setup: A) loaded, B) loaded and masked, C) being tested in solution, and D) top-down perspective.....	13
Fig. 7	Geometry 1e in situ environmental setup: A) loaded, B) loaded and masked, and C) being tested in salt water.....	13
Fig. 8	Final 1a.1 specimen geometry life prediction models.....	15
Fig. 9	Final 1a.2 specimen geometry life prediction models.....	16
Fig. 10	Final 1c specimen geometry life prediction models.....	17
Fig. 11	Final 1d specimen geometry life prediction models.....	18
Fig. 12	Final 1e specimen geometry life prediction models.....	19
Fig. 13	ASTM-F519 type 1d specimen geometry .....	23
Fig. 14	Masking/plating of the 1d specimen geometry.....	25
Fig. 15	Cadmium-plated experimental specimens, type 1d.....	29
Fig. 16	Phase 2 geometry 1d in situ environmental setup: A) loaded, B) loaded and masked, C) being tested in solution, and D) top-down perspective .....	29
Fig. 17	Final Brulin 815 GD life prediction models.....	30
Fig. 18	Final Brulin 1990 GD life prediction models.....	31
Fig. 19	Final Cee Bee 300 LFM life prediction models .....	32
Fig. 20	Final Calla 602 LF life prediction models.....	33
Fig. 21	Final Daraclean 282 life prediction models.....	34
Fig. 22	Final LHE cadmium with Daraclean 282 life prediction models .....	44
Fig. 23	Final Alumiplate with Daraclean 282 life prediction models.....	45
Fig. 24	Final IVD aluminum with Daraclean 282 life prediction models .....	46

Fig. 25	Final Atotech Alkaline LHE Zn-Ni with Daraclean 282 life prediction models .....	47
Fig. 26	Final Dipsol Alkaline LHE Zn-Ni with Daraclean 282 life prediction models .....	48



## List of Tables

---

Table 1	Temper lot quantities .....	6
Table 2	Phase 1 design of experiment conditions matrix .....	8
Table 3	Phase 1 linear portion test matrix .....	9
Table 4	Phase 1 quadratic portion test matrix.....	9
Table 5	Phase 1 confirmation portion test matrix .....	10
Table 6	Phase 2 design of experiment conditions matrix .....	26
Table 7	Phase 2 linear portion test matrix .....	27
Table 8	Phase 2 quadratic portion test matrix.....	27
Table 9	Phase 2 confirmation portion test matrix .....	28
Table 10	Phase 3 design of experiment conditions matrix .....	40
Table 11	Phase 3 linear portion test matrix .....	41
Table 12	Phase 3 quadratic portion test matrix.....	41
Table 13	Phase 3 confirmation portion test matrix .....	42

## Acknowledgments

---

The authors wish to thank Mr Ed Babcock, Mr Stephen Gaydos, and Dr Joseph Osborne of The Boeing Company for fruitful discussions and analysis of the data presented within this work. They were truly a crucial part of the fundamental background and motivation for the development of this work. Mr Richard Green of Green Specialty Service and Mr Craig Willan of Omega Research Inc. are acknowledged for the material specimens and their continuous support of this work. Mr David Kelly of ASKO Processing Inc. and Mr Louie Tran and Mr Bruce Griffin of the Boeing Company provided plating services and supported numerous discussions of cadmium plating. Mr Chad Hogan continuously supported this effort and related efforts through his work on hydrogen embrittlement mitigation of landing gear systems.

## 1. Introduction and Background

---

Solvent substitution for maintenance and overhaul operations of military systems has been a primary environmental concern for many years. Cadmium replacement in these systems has been targeted for decades. Both of these areas have a common obstacle for implementation of any potential alternate. Hydrogen embrittlement is the most predominant unforeseen hurdle since high-strength steels show sensitivity to the phenomena and the source of the hydrogen can be anything within the fabrication process, maintenance practice, or the natural corrosion cycle. Standardized testing on this issue has traditionally stemmed from the aerospace industry where it is a principal focus. Fully understanding the potential for failure is crucial to the decision process on where and when these alternate chemicals and coatings can be safely implemented.

High-strength steel is used on aircraft components, such as landing gear, and the steel is typically cadmium plated to improve the corrosion resistance. Because high-strength steel (ultimate tensile strength [UTS] = 260–300+ ksi) is sensitive to hydrogen embrittlement and subsequent catastrophic failure, precautions need to be taken to ensure that when maintenance activities occur on aircraft components they do not cause embrittlement of the steel. Therefore, aircraft maintenance chemicals (cleaners, deicers, paint strippers, decontamination agents, etc.) are tested per ASTM-F519, Annex A5 (re-embrittlement test methods) to verify that they do not cause hydrogen embrittlement of cadmium-plated high-strength steel.<sup>1</sup>

Re-embrittlement testing has been in use for many years by the different branches of the Department of Defense (DOD) and the aircraft original equipment manufacturers (OEMs), and is carried out with at least 5 different types of ASTM-F519 test specimens and at least 5 different test conditions. This means that there are at least 25 different hydrogen re-embrittlement test methods used in the aerospace industry. The reason for the disparity among re-embrittlement test methods is that at one time there were many different aircraft companies that all developed their own methods to test for hydrogen re-embrittlement. ASTM-F519 Annex A5 became the repository for all of these test methods. Consolidation, or at least a means of comparison, has been a roadblock since inception.

This approach for qualifying aircraft maintenance chemicals in the aerospace industry has been tolerated for many years because cadmium-plated high-strength steel is a very common material used on aircraft. However, efforts are underway to replace cadmium with less hazardous materials and the re-embrittlement test is increasingly a roadblock and source of controversy in the implementation of

cadmium and solvent alternatives. For example, if zinc-nickel (Zn-Ni) is being considered as a replacement for cadmium plating, one of the qualification tests that needs to be carried out before Zn-Ni is implemented is the re-embrittlement test, but which specimen and method are correct? To satisfy all of the DoD and OEM requirements, and to qualify just one maintenance chemical to work with Zn-Ni on high strength steel, many tests with varied parameters are required. Under current conditions, the total amount of testing required to qualify a single cadmium replacement has proven cost and time prohibitive and leaves many questions unanswered when a failed result is achieved.

The ASTM F07 Committee on Aerospace and Aircraft Test Methods has an F07.04 subcommittee on hydrogen embrittlement testing that is responsible for ASTM-F519, and Annex A5 in this specification covers hydrogen re-embrittlement testing of aircraft maintenance chemicals. This subcommittee is very interested in reducing and improving the re-embrittlement tests specified in Annex A5 and wants to consider other test specimen materials. However, to change the test method, it is necessary to develop the data justifying the adoption of the proposed test methods. Several members have taken the time to coordinate and formulate a design of experiment (DoE) aimed at addressing this issue.

Due to the critical nature of catastrophic failure from hydrogen embrittlement on aviation systems, heavy restrictions were placed on the use of alternate chemicals and coatings. Solvents and cadmium coatings have been gradually replaced for more than 20 years in industrial manufacturing and federal maintenance facilities. The replacement chemicals are more environmentally friendly, but are not as inert to the materials as solvents. As such, both private industry and federal agencies have restricted the implementation of these chemicals on some materials. In particular, use on high-strength steel has been scrutinized. Hydrogen, both inherent to the aqueous-based chemicals and emitted during the corrosion cycle, is absorbed by the material. Once absorbed, hydrogen migrates to the largest areas within the metal lattice. These areas can be dislocations, voids, grain boundaries, or simply highly stressed locations. Once the hydrogen tolerance threshold is exceeded for a specific material in a specific application, excess hydrogen migrates to the grain boundaries and accumulates. Eventually, the material separates along the grain boundaries in the area of highest tensile stress. This failure is at a far lower stress than would be the case for a material without excessive hydrogen present, typically levels of 40% to 60% of the material UTS are observed. Levels as low as 10% of the UTS are possible. Accordingly, mandates have required users to bake relieve components subject to these processes to drive the hydrogen out. The bake relief treatments are both time

consuming and labor intensive and therefore both add cost to the cycle. It would be beneficial to determine the material strength level and applications where the alternative chemicals and coatings could be safely used. If materials below a threshold material strength or applied stress do not show susceptibility to hydrogen, then the bake relief treatments could be alleviated for many components.

A 3-phase approach was developed to demonstrate the hydrogen threshold for the applicable chemicals and coatings. The first phase centered on the test material and geometry. Traditionally, hydrogen embrittlement testing has been performed on air-melted 4340 steel with 260–280 ksi strength. It was thought that air-melted steel was the worst case since it would have more internal flaws than vacuum arc re-melted (VAR) aerospace grade steel of the same strength value. The 5 common geometries from ASTM-F519 were evaluated to discern the most susceptible to hydrogen. In the second phase, the most prevalent maintenance chemical cleaners would be evaluated using the geometry and material determined under the first phase. The third phase would then consist of evaluating the most prospective cadmium alternatives in combination with the resulting parameters of the first 2 phases. Obviously not all chemical cleaners and not all cadmium alternatives could be characterized. The emphasis was focused upon the most prevalent chemicals and coatings being used in the aviation industry, where the most impact could be felt from lessening the implementation restrictions.

A DoE approach was used over a range of material strength, load level, and hydrogen-emitting environment for 4340 steel. The load was monitored constantly to determine the precise time to fracture for a specific set of parameters. This allowed comparisons across material strength, applied stress, test solution, or concentration to be drawn. Incorporating the failure time, load, and solution concentration levels into failure models yielded predictive equations over broad parameter ranges. Reliable predictions of hydrogen sensitivity under specific conditions were then realized for each phase. The results of this work provide the rationale for the governing aviation authority of the Army, Aviation and Missile Command/Aviation and Missile Research, Development, and Engineering Center, to relax the current risk assessment to further implement prospective environmentally friendly maintenance chemicals and coatings on aerospace materials in strength applications below that which is assessed in ASTM-F519. This greatly increases the number of applications for which the replacements will be considered, as the models provide the acceptability criteria for the parameters specific to each application.

## **2. Phase 1**

---

### **2.1 Introduction**

---

Phase 1 evaluated hydrogen susceptibility over a range of material strength, load level, and hydrogen-emitting environment (wt% sodium chloride [NaCl]) in 2 different material grades of 4340, while developing life prediction models for each geometry. This demonstrated the comparative susceptibility of each material and geometry with relation to simulated environmental corrosion.

### **2.2 Objective**

---

This phase was designed to utilize a DoE approach to create life prediction models for air-melted SAE-AMS-6415 and vacuum-melted SAE-AMS-6414 (aerospace grade) steel using common ASTM-F519 specimen geometries in combination with load cell measurement and time monitored experiments.<sup>1-3</sup> The data gathered allowed a conclusive determination to be made as to which material and geometry is most sensitive to hydrogen. The results were subsequently used in Phases 2 and 3 to evaluate the most prospective environmentally friendly maintenance chemicals and cadmium alternative coatings that currently have restrictions due to the perceived risk of hydrogen embrittlement.

### **2.3 Materials**

---

The 5 specimen geometries used, fabricated from both AMS 6415 air-melted and AMS 6414 VAR 4340 steel, were manufactured in accordance with the geometries of ASTM-F519 type 1a.1, 1a.2, 1c, 1d, and 1e specimens. These specimens are commonly used by nearly all of the aerospace industry and technical community for conducting hydrogen embrittlement research. They are depicted in Fig. 1.

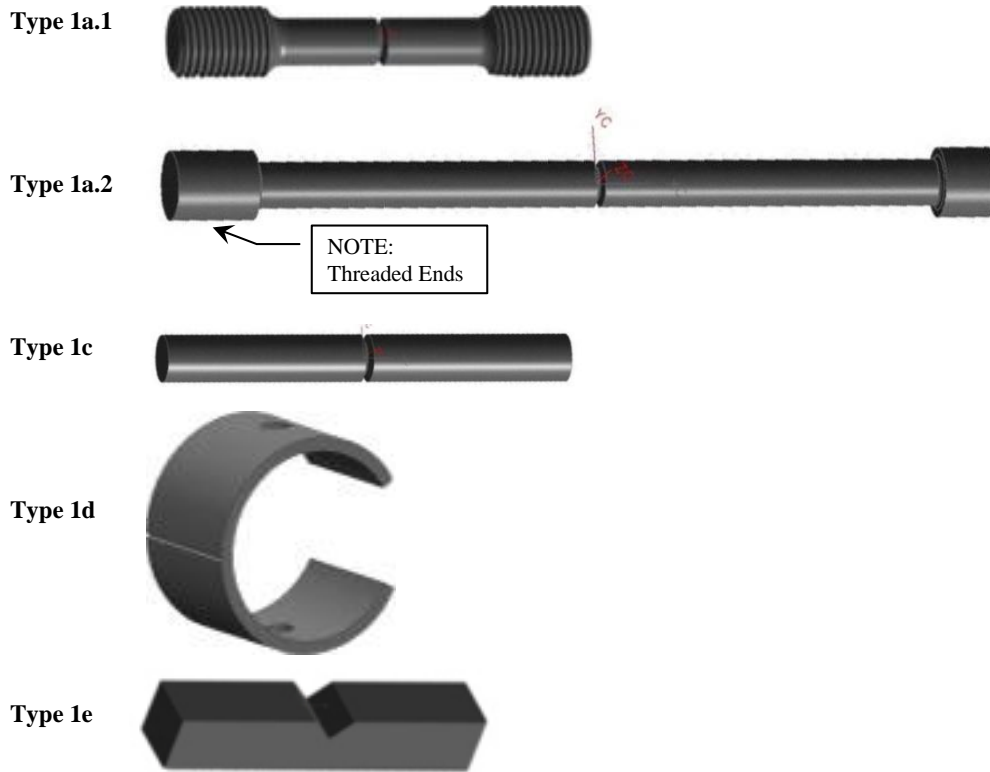


**Fig. 1 ASTM-F519 specimen geometries**

### **2.3.1 Heat Treating**

A critical element in conducting this comparative research across the 5 geometries was to maintain identical material strength. This proved tedious as the stock removal differs on each specimen geometry in blanking and final machining. Additionally, production heat treating proved an imprecise process without tight control. Suppliers were not accustomed to keeping such tight tolerances on their heat-treated product. It was crucial to have the strength level of each specimen in a very narrow range ( $\pm 5$  ksi); otherwise, data variation based on geometry might not be observable in the output. The team constructed a submatrix for the background work. This process entailed certification of a rack-basket, hardening furnace, and tempering furnace by normalizing, hardening, and tempering samples to 280 ksi utilizing small cylindrical buttons for in-process hardness tests and verification tensile samples. Once tested, verified, and certified per mutually agreed parameters, furnaces and ovens had the process frozen for approval. The heat treatments of the actual specimens were completed within 30 days of the date of frozen planning approval. There were 5 heat treatment batches for this work across 5 ASTM-F519 specimen geometries: 1a.1, 1a.2, 1c, 1d, and 1e. Each batch of specimens, T1 through T5, required heat treatment in accordance with the following:

- T1 =  $140 \pm 5$  ksi (135–145 ksi)
- T2 =  $158 \pm 5$  ksi (153–163 ksi)
- T3 =  $210 \pm 5$  ksi (205–215 ksi)
- T4 =  $262 \pm 5$  ksi (257–267 ksi)
- T5 =  $280 \pm 5$  ksi (275–285 ksi)

The specimen counts varied by temper level following the overall DoE. The specimens were heat treated in batches according to their temper lot designation depicted in Table 1. The individual quantities were derived from the DoE matrix further explained in the Phase 1 experimental procedures section (Section 2.4).

- T1 = 30 + 6 tensiles
- T2 = 75 + 6 tensiles
- T3 = 180 + 6 tensiles
- T4 = 75 + 6 tensiles
- T5 = 45 + 6 tensiles

**Table 1 Temper lot quantities**

Temper Lot No.	Strength Target (ksi)	No. of Specimens							
		1a.1	1a.2	1c	1d	1e	Total	+	Tensiles
T1	140	6	6	6	6	6	30	+	6
T2	158	15	15	15	15	15	75	+	6
T3	210	36	36	36	36	36	180	+	6
T4	262	15	15	15	15	15	75	+	6
T5	280	9	9	9	9	9	45	+	6

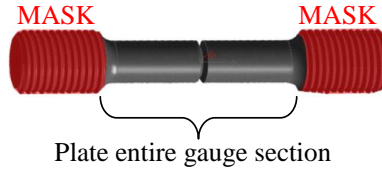
### 2.3.2 Cadmium Plating

The plating requirements were critical since the surface area plated affects both the amount of hydrogen introduced into the sample and the free path out of the sample during hydrogen bake relief. Specimens were supplied in the stress-relieved condition to an aerospace industry approved cadmium plating vendor. The cadmium plating was low hydrogen embrittlement (LHE) cadmium in accordance with MIL-STD-870 Rev. C. Type II, Class 1.<sup>4</sup> The threads were masked and the specimens were postprocessed baked at  $375 \pm 25$  °F within 1 h after plating. Plating requirements were set so that each specimen would have an equivalent surface area to volume ratio during environmental testing, but were largely dependent on the allowable container size for holding the test fluid. The

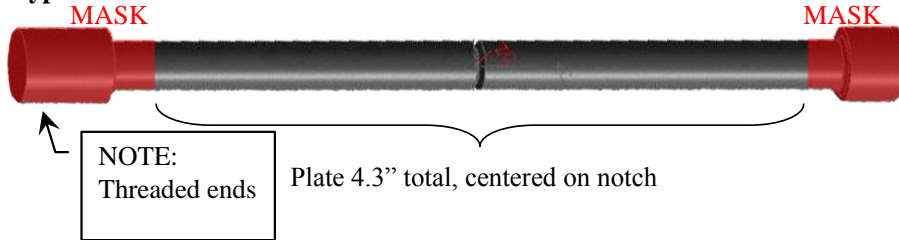


masking requirements also stipulated that no fluid would contact bare unplated steel during re-embrittlement testing. The plated area of the specimens was in accordance with the Fig. 2.

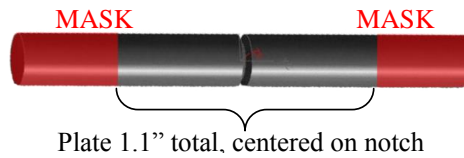
**Type 1a.1**



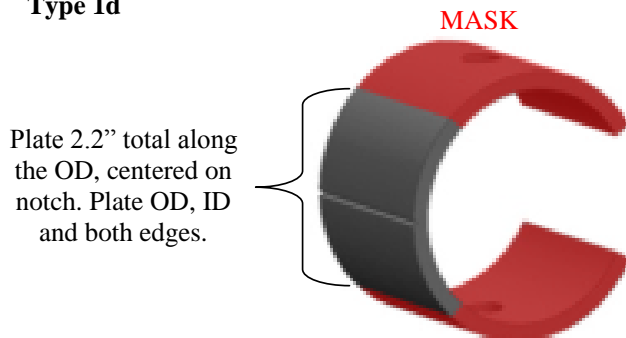
**Type 1a.2**



**Type 1c**



**Type 1d**



**Type 1e**

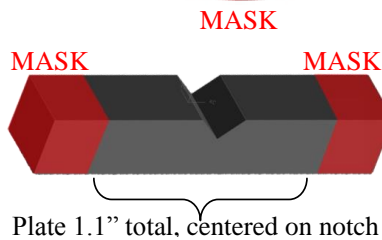


**Fig. 2 Masking/plating of the 5 specimen geometries**

## 2.4 Experimental Procedures

### 2.4.1 Design of Experiment

This approach was used over a range of material strength for both grades of 4340 steel, load level, and hydrogen environment. The 5 geometries were tested while load levels were monitored to determine a precise time to fracture at specific percentages of notch fracture strength (NFS), specific material strengths (heat treat tempers T1–T5), and specific hydrogen-emitting environment (wt% NaCl). Contrary to the existing standard, greater information was gleaned beyond the result of a pass/fail test. Once the failure time, load, and stress level data were incorporated into DoE failure models, predictive equations over the broad ranges were developed.

The DoE focused on 3 variables for the 5 geometries (ASTM-F519 types 1a.1, 1a.2, 1c, 1d, and 1e). The control variables were selected from risk reduction and ruggedness leveraged efforts conducted by The Boeing Company with the assistance of the US Army Research Laboratory (ARL). The 5 geometries were selected from the ASTM-F519 test method. Table 2 presents the range of test conditions for the 5 ASTM-F519 test geometries researched.

**Table 2 Phase 1 design of experiment conditions matrix**

Condition	$-\alpha$	$-$	$0$	$+$	$+\alpha$
Strength (ksi)	140	158	210	262	280
Test load (% NFS)	40	45	60	75	95
NaCl concentration (wt% NaCl)	1.25E-05	0.01	0.50	2.36	3.5

Below 140 ksi, steel is generally accepted as not being sensitive to hydrogen, which set the lower limit for strength. NaCl was not used at 0% concentration, essentially completely deionized water, since the working group had experience that deionized water is actually severely corrosive and a very harsh environment for steel. It is also not a real world environment. The level chosen reflects a real world zero amount of electrolyte.

The DoE approach was refined with preliminary ruggedness and risk reduction efforts at Boeing-Mesa, with technical assistance from Boeing-St. Louis, Boeing-Seattle, and ARL. Typical of DoEs, it consisted of 3 test portions, a linear portion, a quadratic portion, and a confirmation portion. The example matrix is presented in Tables 3–5 with the condition values corresponding to Table 2. These experiments aided the development of appropriate boundary conditions for the larger effort.

**Table 3 Phase 1 linear portion test matrix**

Repeat Entire Matrix 2× for 1a.1, 1a.2, 1c, 1d, and 1e	Run ID	A	B	C	Run Order
		Strength (ksi)	Test Load (% NFS)	NaCl Conc. (wt% NaCl)	
Linear portion	L1	–	–	–	Random
	L2	–	–	+	
	L3	–	+	–	
	L4	–	+	+	
	L5	+	–	–	
	L6	+	–	+	
	L7	+	+	–	
	L8	+	+	+	
Center points	C1	0	0	0	
	C2	0	0	0	
	C3	0	0	0	
	C4	0	0	0	
	C5	0	0	0	
	C6	0	0	0	

**Table 4 Phase 1 quadratic portion test matrix**

Repeat Q1–Q6 5× for 1a.1, 1a.2, 1c, 1d and 1e	Run ID	A	B	C	Run Order
		Strength (ksi)	Test Load (% NFS)	NaCl Conc. (wt% NaCl)	
Not replicated	C7	0	0	0	First
Quadratic portion	Q1	$+\alpha$	0	0	Random
	Q2	$-\alpha$	0	0	
	Q3	0	$+\alpha$	0	
	Q4	0	$-\alpha$	0	
	Q5	0	0	$+\alpha$	
	Q6	0	0	$-\alpha$	
Not replicated	C8	0	0	0	Last

**Table 5 Phase 1 confirmation portion test matrix**

	Run ID	A	B	C	Run Order
		Strength (ksi)	Test Load (% NFS)	NaCl Conc. (wt% NaCl)	
Confirmation portion	1				
	2				
	3				
	4				
	5				
	6				
	7				
	8	Varied depending on outcome of linear, center, and quadratic			Random
	9				
	10				
	11				
	12				
	13				
	14				
	15				
	16				

After the linear and center point data runs are completed, initial calculations were made for the predictive model equations. Those initial models were utilized to choose confirmation runs to be researched. The confirmation run results were then incorporated into refining the initial working model.

#### 2.4.2 Specimens, Environment, and Loading

Air-melted and VAR aerospace grade 4340 steel samples in 5 ASTM-F519 geometries and heat treated to 5 different material strengths, as previously described, were tested in accordance with ASTM-F519. The specimens demonstrated adequate hydrogen sensitivity of the material. The cadmium-plated specimens used for these experiments are depicted in Fig. 3. The axially loaded specimens (geometries 1a.1 and 1a.2) were tested on Instron or MTS uniaxial load mechanical test frames; the 1c and 1e specimens were loaded with double cantilever bending fixtures; and the 1d specimens were directly loaded with nut and bolt. The loads were monitored with the load cells on the mechanical test frames and via loading rings installed in the load path for the other geometries. The load cells and load rings were calibrated prior to the experiments. For this phase, loads were applied as a percentage (45%–95%) of the calculated 100% NFS determined for each geometry. Ten specimens were utilized to calculate the average 100% NFS with the identical fixturing applied during the experiments. Ten specimens from each group were loaded to failure. The experimental loading

was then applied as a percentage of this determined average NFS failure load. Loads were recorded from the mechanical test frames for geometries 1a.1 and 1a.2, and with data sampling hardware and software for the other geometries. Figures 4–7 depict the in situ test apparatus for the experiments.

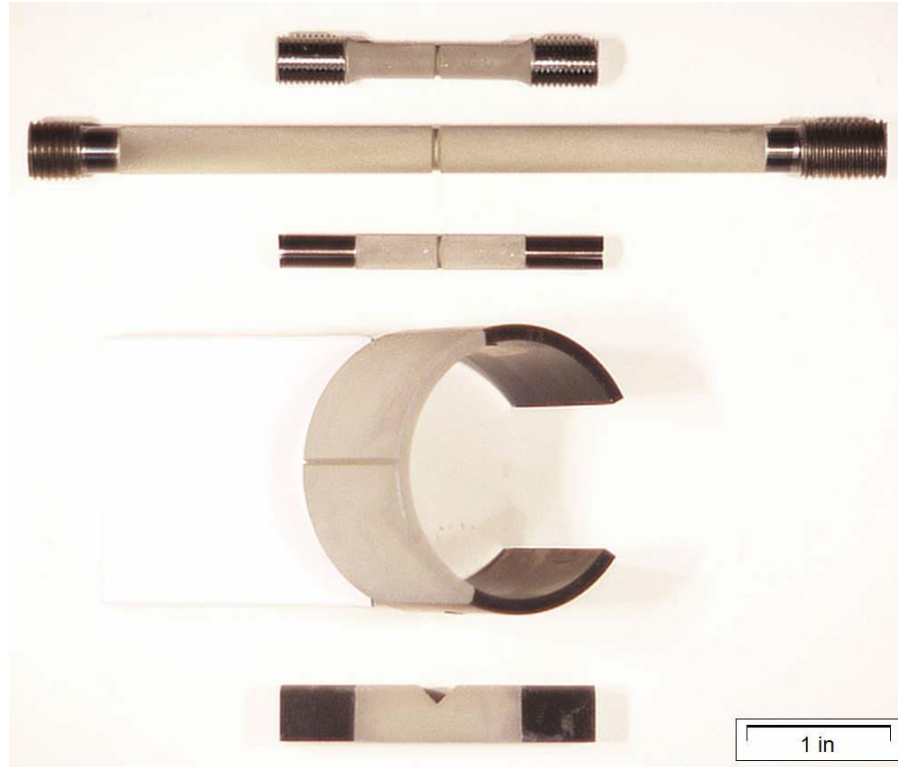


**Fig. 3 Cadmium-plated experimental specimens 1a.1, 1a.2, 1c, 1d, and 1e (top to bottom)**



**Fig. 4** Geometry 1a.1 and 1a.2 in situ environmental setup: A) empty container, B) sample in the cup, C) sample loaded onto the mechanical test frame, and D) sample being tested in solution

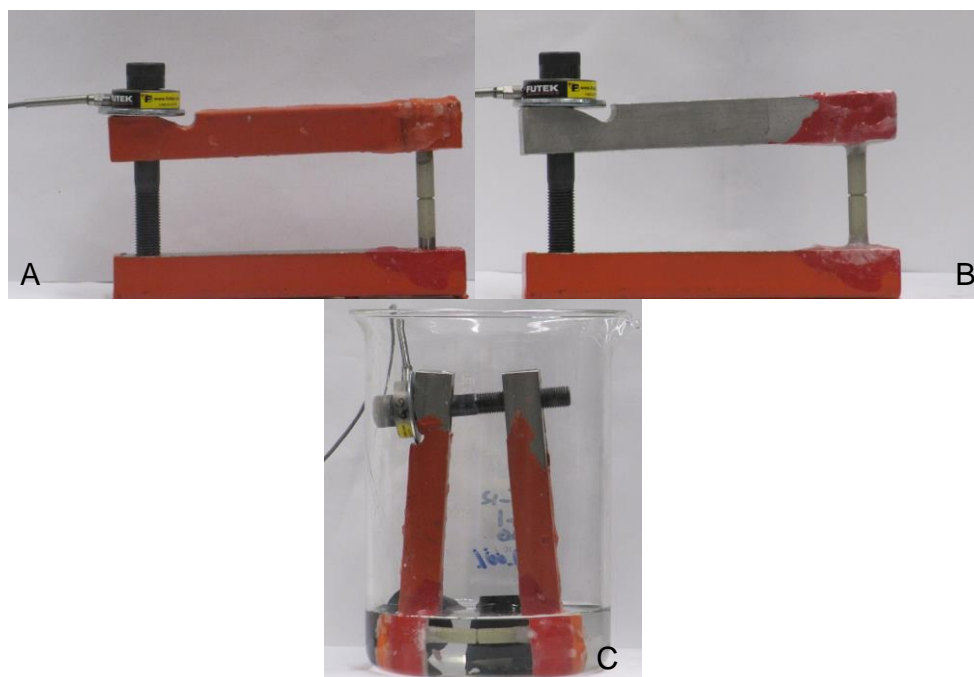


**Fig. 5** Geometry 1c in situ environmental setup: A) loaded, B) loaded and masked, and C) being tested in solution

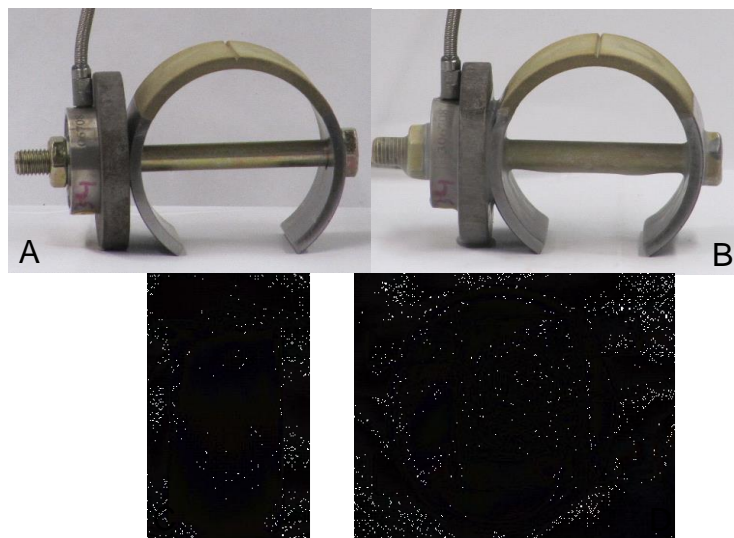


**Fig. 6** Geometry 1d in situ environmental setup: A) loaded, B) loaded and masked, C) being tested in solution, and D) top-down perspective

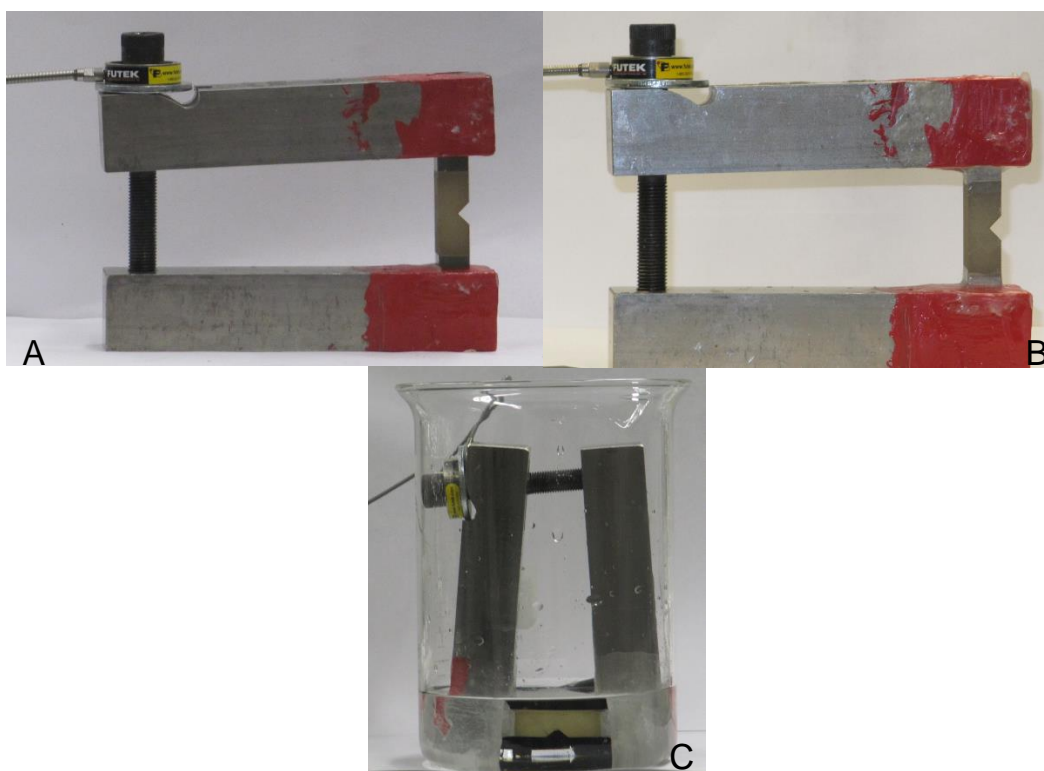


**Fig. 7** Geometry 1e in situ environmental setup: A) loaded, B) loaded and masked, and C) being tested in salt water

The samples were cadmium plated at Asko Processing, Inc., Seattle, WA, in accordance with MIL-STD-870 Rev. C. Type II, Class 1. Plated samples were sensitivity tested in accordance with ASTM-F519. Cadmium plating process embrittlement testing involved loading 3 T5 samples from each geometry to 75% of their NFS and holding for 200 h in air. These specimens did not fail, and thus insured that the plating process did not embrittle the specimens.

The specimens were masked so that only the cadmium-plated surface contacted the test solution. The solution used was NaCl in deionized water in 5 different concentrations:  $1.25 \times 10^{-5}$  wt%, 0.01 wt%, 0.5 wt%, 2.36 wt%, and 3.5 wt% in accordance with Table 2. The volume of NaCl solution for each sample geometry was calculated to ensure that each geometry had the same ratio of cadmium-plated surface area to solution volume (if this volume was not enough to submerge the samples adequately, clean inert material was added to displace solution to submerge the samples to the correct level. The loaded specimens were then immersed in the test solution for the duration of the experiment. Specimens were removed either upon failure or after 168 h of sustained load without failure.

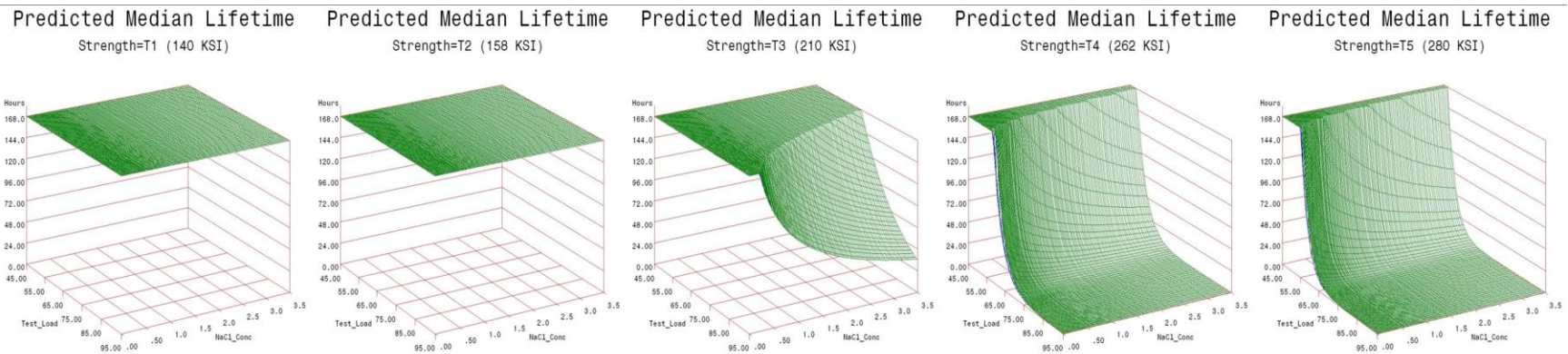
As stated previously, upon conclusion of the linear, center, and quadratic test runs, preliminary life prediction models were created. These models were then used in the confirmation test portion of the matrix to choose appropriate parameters to both enhance and verify the model. Final life prediction equations and 3-dimensional (3-D) models were created after the incorporation of the confirmation data.

## **2.5 Results**

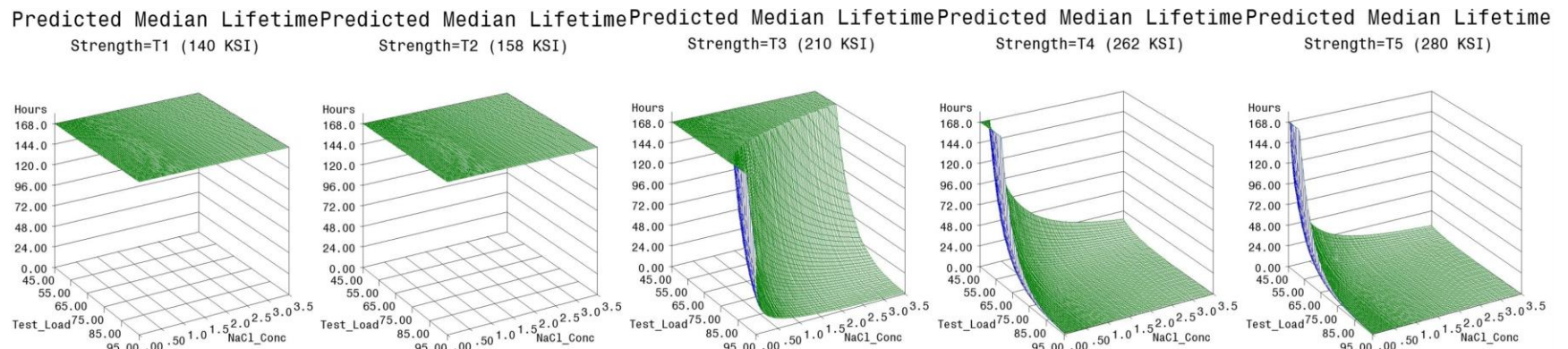
---

The final life prediction models for each geometry and material are presented in Figs. 8–12 for type 1a.1, 1a.2, 1c, 1d, and 1e, respectively. The models, for each respective geometry and material, did not vary significantly from the preliminary set, thus verifying the initial prediction and methods. The x and y axes are applied load and NaCl concentration, respectively, while the z or vertical axis represents time to failure. The flat portions of the top of the 3-D graphs indicate no failure within 168 h. The “safe-zone” would therefore be the area below the graphs, where the load or NaCl concentration was too low to cause failure.





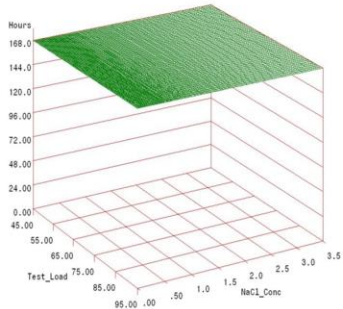
## Air-melt 4340 - AMS-6415



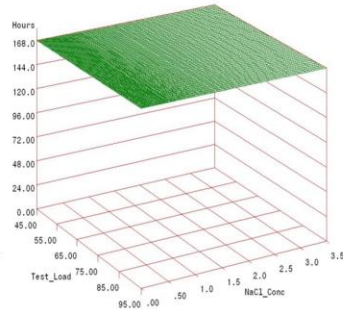
## Aerospace 4340 - AMS-6414

Fig. 8 Final 1a.1 specimen geometry life prediction models

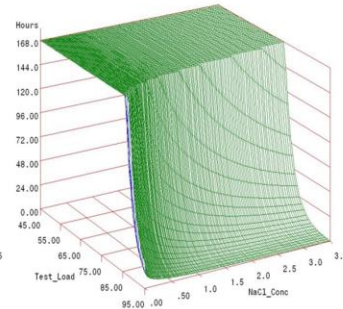
Predicted Median Lifetime  
Strength=T1 (140 KSI)



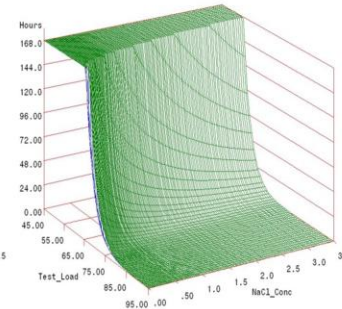
Predicted Median Lifetime  
Strength=T2 (158 KSI)



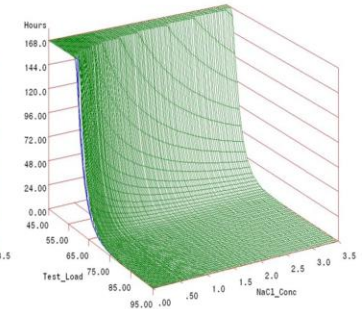
Predicted Median Lifetime  
Strength=T3 (210 KSI)



Predicted Median Lifetime  
Strength=T4 (262 KSI)

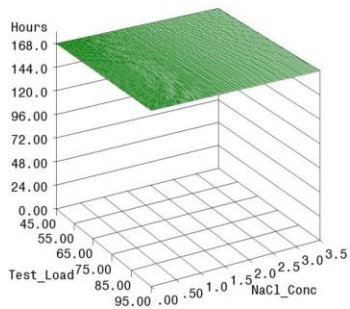


Predicted Median Lifetime  
Strength=T5 (280 KSI)

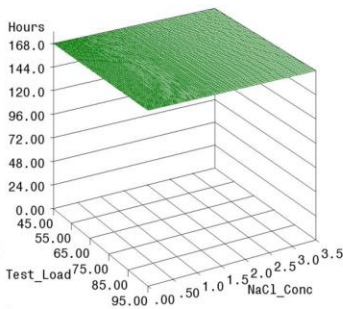


## Air-melt 4340 - AMS-6415

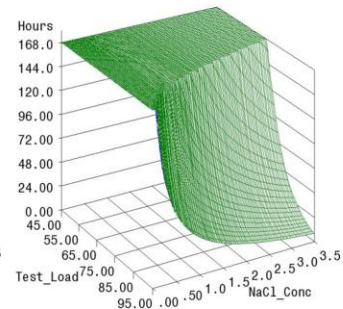
Predicted Median Lifetime  
Strength=T1 (140 KSI)



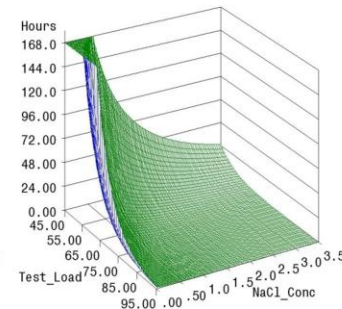
Predicted Median Lifetime  
Strength=T2 (158 KSI)



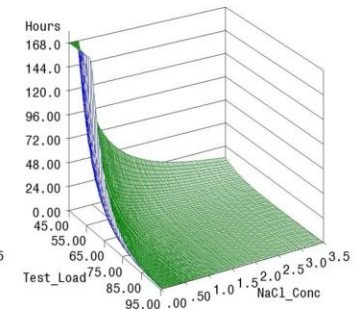
Predicted Median Lifetime  
Strength=T3 (210 KSI)



Predicted Median Lifetime  
Strength=T4 (262 KSI)



Predicted Median Lifetime  
Strength=T5 (280 KSI)

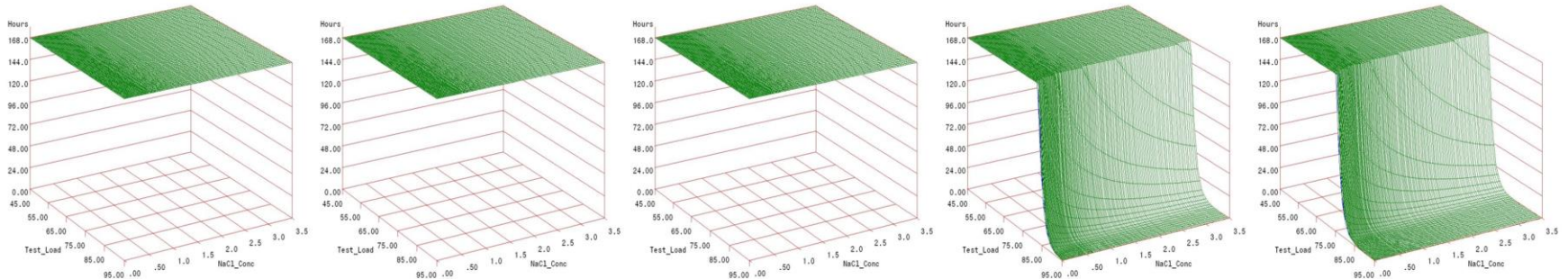


## Aerospace 4340 - AMS-6414

Fig. 9 Final 1a.2 specimen geometry life prediction models

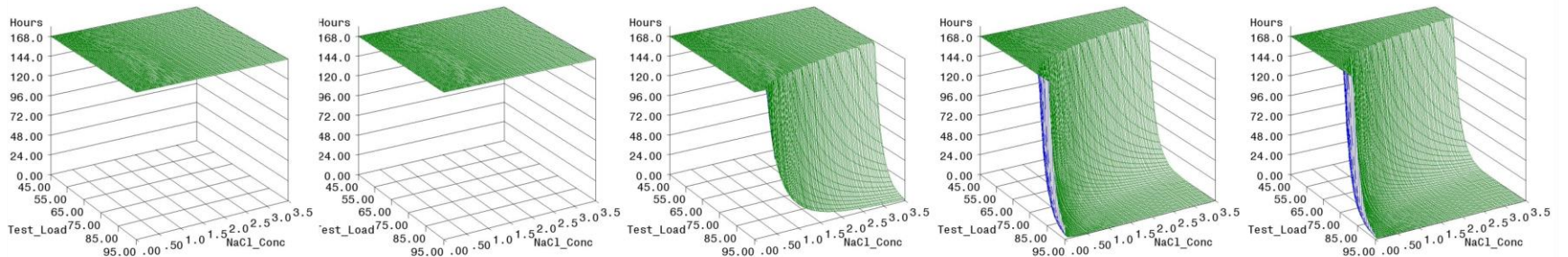


Predicted Median Lifetime  
Strength=T1 (140 KSI)      Predicted Median Lifetime  
Strength=T2 (158 KSI)      Predicted Median Lifetime  
Strength=T3 (210 KSI)      Predicted Median Lifetime  
Strength=T4 (262 KSI)      Predicted Median Lifetime  
Strength=T5 (280 KSI)



Air-melt 4340 - AMS-6415

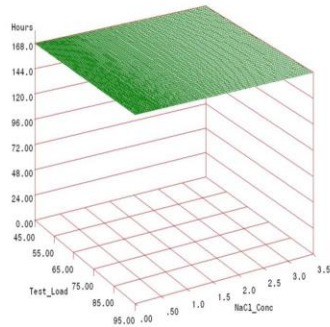
Predicted Median Lifetime  
Strength=T1 (140 KSI)      Predicted Median Lifetime  
Strength=T2 (158 KSI)      Predicted Median Lifetime  
Strength=T3 (210 KSI)      Predicted Median Lifetime  
Strength=T4 (262 KSI)      Predicted Median Lifetime  
Strength=T5 (280 KSI)



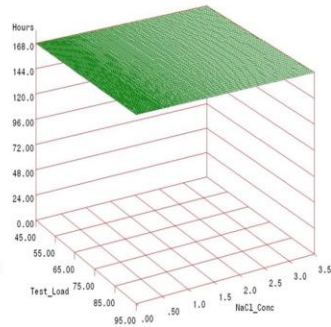
Aerospace 4340 - AMS-6414

Fig. 10 Final 1c specimen geometry life prediction models

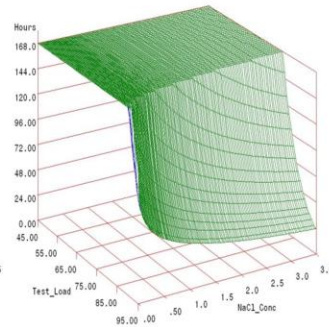
Predicted Median Lifetime  
Strength=T1 (140 KSI)



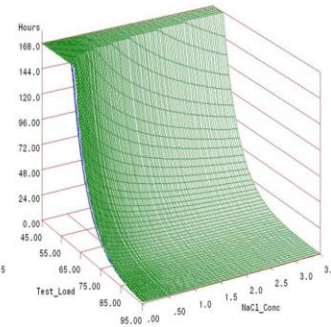
Predicted Median Lifetime  
Strength=T2 (158 KSI)



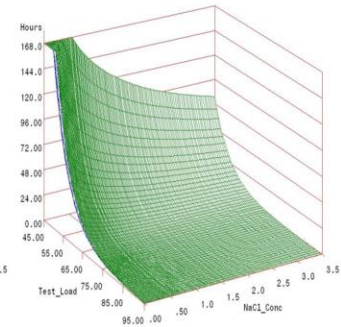
Predicted Median Lifetime  
Strength=T3 (210 KSI)



Predicted Median Lifetime  
Strength=T4 (262 KSI)

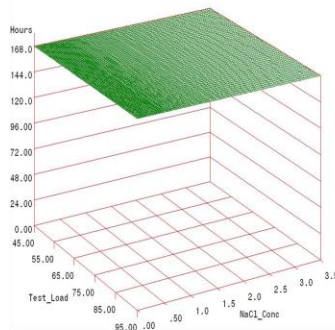


Predicted Median Lifetime  
Strength=T5 (280 KSI)

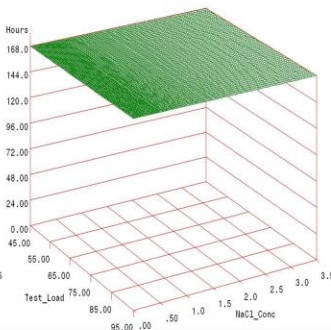


## Air-melt 4340 - AMS-6415

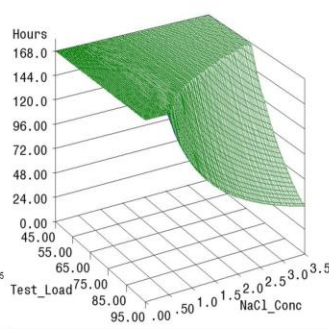
Predicted Median Lifetime  
Strength=T1 (140 KSI)



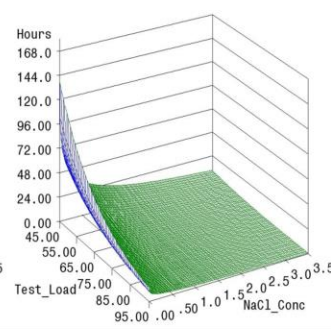
Predicted Median Lifetime  
Strength=T2 (158 KSI)



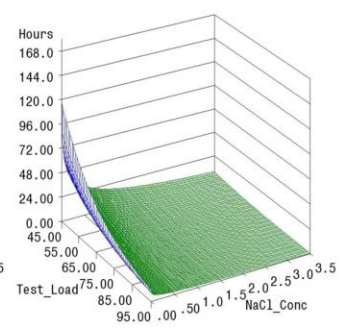
Predicted Median Lifetime  
Strength=T3 (210 KSI)



Predicted Median Lifetime  
Strength=T4 (262 KSI)



Predicted Median Lifetime  
Strength=T5 (280 KSI)

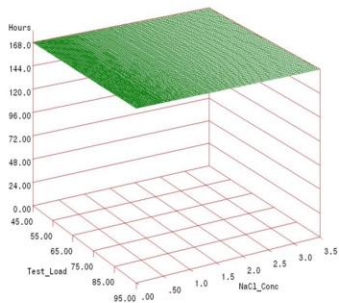


## Aerospace 4340 - AMS-6414

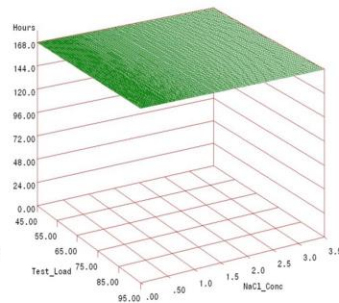
Fig. 11 Final 1d specimen geometry life prediction models



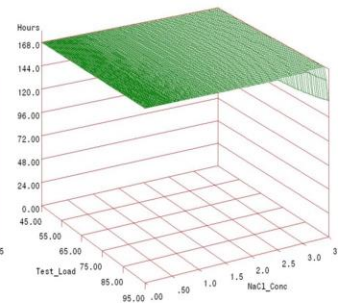
Predicted Median Lifetime  
Strength=T1 (140 KSI)



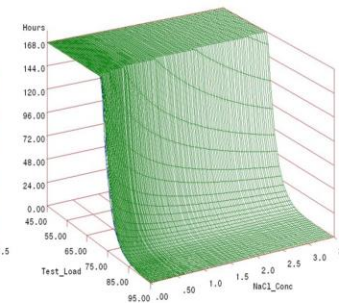
Predicted Median Lifetime  
Strength=T2 (158 KSI)



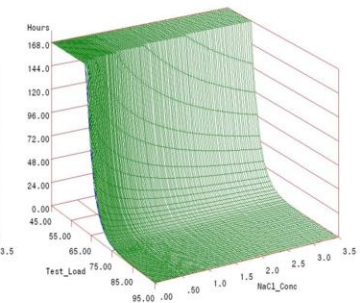
Predicted Median Lifetime  
Strength=T3 (210 KSI)



Predicted Median Lifetime  
Strength=T4 (262 KSI)

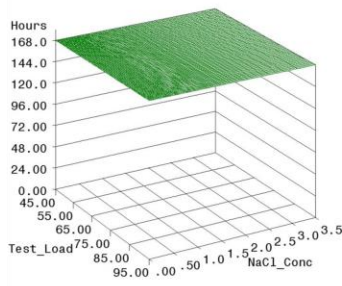


Predicted Median Lifetime  
Strength=T5 (280 KSI)

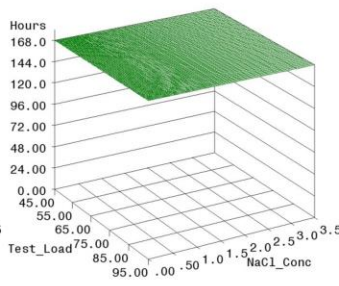


## Air-melt 4340 - AMS-6415

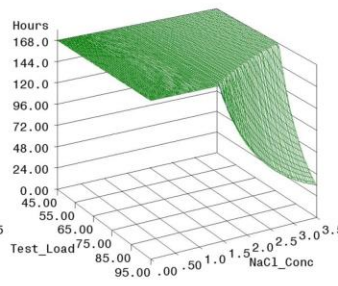
Predicted Median Lifetime  
Strength=T1 (140 KSI)



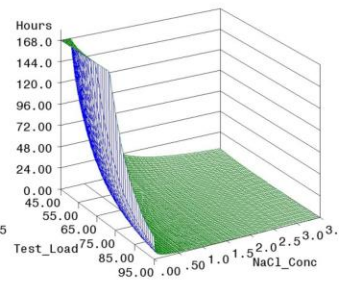
Predicted Median Lifetime  
Strength=T2 (158 KSI)



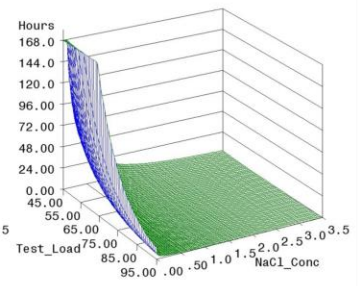
Predicted Median Lifetime  
Strength=T3 (210 KSI)



Predicted Median Lifetime  
Strength=T4 (262 KSI)



Predicted Median Lifetime  
Strength=T5 (280 KSI)



## Aerospace 4340 - AMS-6414

Fig. 12 Final 1e specimen geometry life prediction models

## 2.6 Discussion

---

It was interesting to discover that air-melted AMS-6415 steel was more tolerant than aerospace grade AMS-6414 steel. It has long been thought that air-melted steel was the weakest link. Indeed, it has lower tensile strength at equivalent hardness. Intuitively this makes some sense, since hardness is determined in a compression test, while tensile strength is performed in tension. The weak inclusion points would most likely reveal themselves preferentially in tension. The school of thought in hydrogen sensitivity is that if you test the worst case in a specific environment and your material survives, then all other cases will not fail. Because air-melted 4340 steel is known to be inferior to aerospace grade 4340 steel, it was used as the performance test material.

Across all geometries, it can be observed in the data that air-melted steel demonstrated more tolerance to hydrogen. This was not expected. All other conditions in the testing protocol were identical. The environment and the loading method were the same; the heat treatment was performed at the same time in the same ovens. The only difference was the material grade of the steel. The case may be made that the cleanliness of aerospace grade steel removes the flaws in the atomic lattice where hydrogen migrates. The less imperfections that the lattice has, the less distributed the damaging hydrogen is since it has nowhere to hide. If one assumes that an equivalent amount of hydrogen enters both materials under similar conditions, then one must conclude that the flaws within the air-melted grade lower the sensitivity of that material to hydrogen since each flaw has the ability to hold some hydrogen as a trap. In the aerospace material with limited inclusions, the hydrogen has nowhere to be absorbed and hide, and therefore migrates to the next largest site, the grain boundaries. When the hydrogen concentration at a load-stressed area goes beyond a critical threshold, the grain boundaries tear apart. This is why hydrogen embrittlement failures exhibit blocky brittle fracture surfaces representative of individual grain boundaries.

Since DoE predictive models had never been attempted before to assess hydrogen sensitivity, the results were extremely satisfying. The predictive models express hydrogen sensitivity in terms of applied load, material strength, and hydrogen environment. In this case, the hydrogen environment is a representation of the natural environmental corrosion cycle. In terms of NaCl salt concentration, 3.5% is widely accepted to be the worst-case scenario for corrosion of steel. Values higher than 3.5% actually result in a lower corrosion rate. The time duration, 168 h (1 week), is above that which is accepted as the lifetime cutoff for service environments, 150 h. Essentially, these data suggest that if the material

demonstrates no hydrogen sensitivity in a 3.5% salt concentration environment for 168 h at a specific strength and applied load combination, then it should not be expected to fail in a lifetime of service exposure in our natural environment at that strength and applied load level. The “safe zone” in the graphical representation of the models is the area below the curves.

A comparison with all of the models across test geometry showed that the 3.5% NaCl is not a severe enough environment to cause hydrogen embrittlement at or below the 158-ksi strength level. All of the “T1, 140-ksi” and “T2, 158-ksi” strength levels are flat, showing no sensitivity. This does not mean that in an environment that emits more hydrogen, no sensitivity would be expected. The converse is actually true. Industrial processes such as electroplating or acidic or alkaline cleaning would certainly be expected to show sensitivity to hydrogen at or below the 158-ksi material strength level.

Although varying performance can be observed across test geometry, the trends are in agreement. The sensitivity increases with material strength level, applied load, and to a lesser degree, with NaCl concentration. All of these trends are in line with traditional expectations. While material strength level is typically given consideration with regard to hydrogen sensitivity, applied load is often forgotten. Residual stresses from forming, quenching, or assembly can often reach 40%–45% of the UTS. This is important to remember since these life prediction models show sensitivity beginning at or even below that region. This supports traditional findings where components sometimes break on the shelf while waiting to be placed in service. When combined with a design stress or in-service applied stress, catastrophic failure is much more likely to occur. The degree of heightened sensitivity from applied stress was unknown before now, since it has never been investigated.

It can also be observed in the data that the type 1d specimen geometry shows the highest sensitivity. It has the highest stress intensity, stemming from the smallest notch root radius. It also has historically performed in comparative tests with heightened sensitivity. While this test geometry may not be representative of every application in terms of stress intensity, one would be able to apply a factor of safety to this life prediction model and have confidence that a similar application would not fail due to hydrogen embrittlement. All the models have similar trends, but a risk analysis would likely be developed from a worst-case and not middle-of-the-pack performance. The 1d geometry is also a self-loading geometry, so it is conducive to testing in various environments since no mechanical test frame is needed. This specimen geometry will be used in the subsequent maintenance fluid and coatings phases evaluating hydrogen sensitivity.

## 2.7 Conclusions

---

The following conclusions can be drawn from the data developed and discussion of this phase.

- Life prediction models were developed that accurately represent the expected hydrogen sensitivity over the range of parameters explored for air-melted and aerospace grade 4340 steel.
- Air-melted 4340 steel has less sensitivity to hydrogen than aerospace grade 4340 steel.
- The trends observed in the data were reasonably consistent across all test geometries. Sensitivity increases with applied load, material strength, and to a lesser degree, NaCl concentration.
- Applied stress has the most direct effect on hydrogen sensitivity, while material strength is a close second. Increasing the value of either parameter directly heightens the sensitivity to hydrogen.
- Air-melted and aerospace 4340 steel do not appear susceptible to hydrogen absorbed from environmental corrosion below the 160-ksi strength level.
- High residual stress levels (40%–50% of UTS) are capable of causing hydrogen embrittlement without further applied system stresses.
- The type 1d test geometry proved the most sensitive to hydrogen and also conducive to testing multiple specimens in various environments without requiring test load frames.

## 3. Phase 2

---

---

### 3.1 Introduction

---

In this phase, 5 prominently used solvent substitute maintenance chemicals; Brulin 815 GD, Brulin 1990 GD, Cee Bee 300 LFM, Calla 602 LF, and Daraclean 282 were tested to mimic the industrial manufacturing and maintenance cycle. The DoE approach was used to vary parameters over a range of material strength, load level, and maintenance cleaning solution concentration for aerospace grade (SAE-AMS-6414) 4340 steel. The cadmium-plated ASTM-F519, type 1d geometry was employed while monitoring load to determine the precise time to fracture for the specific set of parameters. This allowed comparisons across



material strength, applied load, and test solution concentration to be drawn. Incorporating the failure time, load, and stress levels into failure models yielded predictive equations over broad parameter ranges. Reliable predictions of hydrogen sensitivity under specific conditions were then realized for each coating.

### 3.2 Objective

---

This phase was designed to utilize a DoE approach to create life prediction models for VAR steel, SAE-AMS-6414.<sup>2</sup> The cadmium-plated ASTM-F519 type 1d specimen geometry in combination with load cell measurement and time monitored experiments was employed.<sup>1</sup> This phase evaluated the most prospective, prominent maintenance chemicals that currently have their use limited via the perceived risk of hydrogen embrittlement. Demonstrating that these chemicals have safe zones below threshold material strengths and load levels provide the rationale to relax the current risk assessment baking requirements to further their implementation in the manufacturing and maintenance cycle on aerospace materials. This should also greatly increase the applications for which these solvent substitute chemicals will be considered, as the models provide the acceptability criteria for the relevant parameters specific to each application.

### 3.3 Materials

---

The type 1d c-ring specimen geometry used in this phase was fabricated from SAE-AMS-6414 VAR steel and was manufactured in accordance with ASTM-F519. These specimens were determined in Phase 1 to have the highest sensitivity to hydrogen when investigating the effects of steel cleanliness (aerospace grade 4340 versus air-melted 4340 steel). The specimen is depicted in Fig. 13.



**Fig. 13** ASTM-F519 type 1d specimen geometry

### **3.3.1 Heat Treating**

As in Phase 1, it was crucial to have the strength level of each specimen in a very narrow range ( $\pm 5$  ksi); otherwise, data variation based on geometry might not be observable in the output. The team constructed a submatrix for the background work. This process entailed certification of a rack-basket, hardening furnace, and tempering furnace by normalizing, hardening, and tempering samples to 280 ksi utilizing small cylindrical buttons for in-process hardness tests and verification tensile samples. Once tested, verified, and certified per mutually agreed parameters, furnaces and ovens had the process frozen for approval. The heat treatments of the actual specimens were completed within 30 days of the date of frozen planning approval. There were 5 heat treatment batches for this work. Each batch of specimens, T1 through T5, required heat treatment in accordance with the following:

- T1 =  $210 \pm 5$  ksi (205–215 ksi)
- T2 =  $220 \pm 5$  ksi (215–225 ksi)
- T3 =  $245 \pm 5$  ksi (240–250 ksi)
- T4 =  $270 \pm 5$  ksi (265–275 ksi)
- T5 =  $280 \pm 5$  ksi (275–285 ksi)

The specimen counts varied by temper level following the overall DoEs. The individual quantities were derived from the DoE matrix further explained in the Phase 2 experimental procedures section (Section 3.4).

- T1 = 30 + 6 tensiles
- T2 = 75 + 6 tensiles
- T3 = 180 + 6 tensiles
- T4 = 75 + 6 tensiles
- T5 = 45 + 6 tensiles

### **3.3.2 Maintenance Chemicals**

There were 5 maintenance chemicals, used for aqueous degreasing as a solvent substitute, selected for this phase. The most prospective prominently used solvent substitutes for cleaning were selected.

- 1) **Brulin 815 GD:** An alkaline, pH 12 (concentrate) maintenance chemical cleaner designed for the aerospace industry to be used at 5%–30% concentration at 170 °F in immersion wash applications.
- 2) **Brulin 1990 GD:** An alkaline, pH 11.3 (concentrate) maintenance chemical cleaner designed for the aerospace industry to be used at 3%–15% concentration at 170 °F in spray wash applications.
- 3) **Cee Bee 300 LFM:** An alkaline, pH 11.5 (concentrate) maintenance chemical cleaner designed for the aerospace industry to be used at 5%–20% concentration at 160 °F in spray wash applications.
- 4) **Calla 602 LF:** An alkaline, pH 8.0 (concentrate) maintenance chemical cleaner designed for the aerospace industry to be used at 5% concentration at 160 °F.
- 5) **Daraclean 282:** An alkaline, pH 12.5 (concentrate) maintenance chemical cleaner designed for the aerospace industry to be used at 3%–25% concentration at 180 °F.

The cadmium plating requirements were critical since the surface area plated affects both the amount of hydrogen introduced into the sample and the free path out of the sample during hydrogen bake relief. Specimens were supplied in the stress-relieved condition to an aerospace industry–approved LHE cadmium plating vendor. The ends were masked, specimens were plated, and then postprocess baked at  $375 \pm 25$  °F within 1 h after plating. The masking requirements were set such that no fluid would contact bare unplated steel during re-embrittlement testing. The plated area of the 1d specimens was in accordance with the Fig. 14.

#### Type 1d

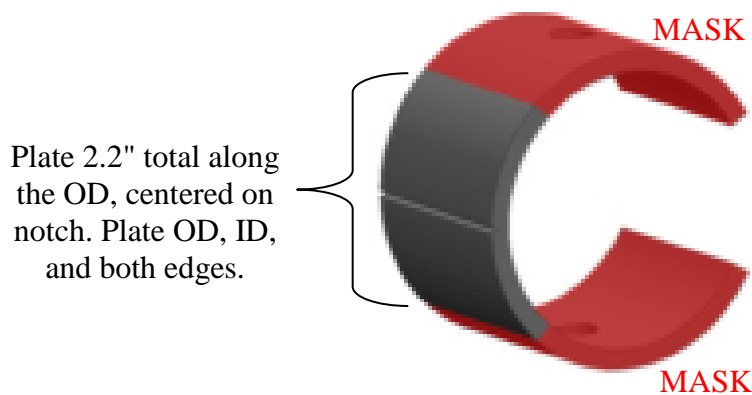


**Fig. 14 Masking/plating of the 1d specimen geometry**

### 3.4 Experimental Procedures

#### 3.4.1 Design of Experiment

This DoE approach was used over a range of material strength, load level, and hydrogen environment. The specimens were tested while load levels were monitored to determine a precise time to fracture at specific percentages of NFS, specific material strengths (heat treat tempers T1–T5), and specific hydrogen-emitting environment (maintenance chemical vol%). Contrary to the existing standard, greater information was gleaned beyond the result of a pass/fail test. Once the failure time, load, and stress level data were incorporated into DoE failure models, predictive equations over the broad ranges were developed.

The DoE focused on 3 variables. The control variables were selected from risk reduction and ruggedness leveraged efforts conducted by The Boeing Company with the assistance of ARL. Table 6 presents the range of test conditions for the test geometry researched.

**Table 6 Phase 2 design of experiment conditions matrix**

<b>Condition</b>	<b>–<math>\alpha</math></b>	<b>–</b>	<b>0</b>	<b>+</b>	<b>+<math>\alpha</math></b>
Strength (ksi)	210	220	245	270	280
Test load (% NFS)	45	55	70	85	95
Maintenance chemical vol%	2	4.5	17.3	30	34.5

The DoE approach was refined with preliminary ruggedness and risk reduction efforts at Boeing-Mesa, with technical assistance from Boeing-St. Louis, Boeing-Seattle, and ARL. It was found that the material did not show susceptibility in the chemicals below 210 ksi. The maintenance chemicals were not used at concentrations near 0%, essentially completely deionized water, since the working group had experience that deionized water is actually severely corrosive and a very harsh environment for steel. It is also not a real-world environment. Typical of DoEs, it consisted of 3 test portions: a linear portion, a quadratic portion, and a confirmation portion. The example matrix is as presented in Tables 7–9 with the condition values corresponding to Table 6. These experiments aided the development of appropriate boundary conditions for the larger effort.

**Table 7 Phase 2 linear portion test matrix**

Repeat Entire Matrix 2×	Run ID	A	B	C	Run Order
		Strength (ksi)	Test Load (% NFS)	Daraclean (wt%)	
Linear portion	L1	–	–	–	Random
	L2	–	–	+	
	L3	–	+	–	
	L4	–	+	+	
	L5	+	–	–	
	L6	+	–	+	
	L7	+	+	–	
	L8	+	+	+	
Center points	C1	0	0	0	
	C2	0	0	0	
	C3	0	0	0	
	C4	0	0	0	
	C5	0	0	0	
	C6	0	0	0	

**Table 8 Phase 2 quadratic portion test matrix**

Repeat Q1–Q6 5×	Run ID	A	B	C	Run Order
		Strength (ksi)	Test Load (% NFS)	Daraclean (wt%)	
Not replicated	C7	0	0	0	First
Quadratic portion	Q1	+ $\alpha$	0	0	Random
	Q2	– $\alpha$	0	0	
	Q3	0	+ $\alpha$	0	
	Q4	0	– $\alpha$	0	
	Q5	0	0	+ $\alpha$	
	Q6	0	0	– $\alpha$	
Not replicated	C8	0	0	0	Last

**Table 9 Phase 2 confirmation portion test matrix**

	Run ID	A	B	C	Run Order
		Strength (ksi)	Test Load (% NFS)	Daraclean (wt%)	
Confirmation portion	1				
	2				
	3				
	4				
	5				
	6				
	7				
	8	Varied depending on outcome of linear, center, and quadratic			Random
	9				
	10				
	11				
	12				
	13				
	14				
	15				
	16				

After the linear and center point data runs were completed, initial calculations were made for the predictive model equations. Those initial models were utilized to choose confirmation runs to be researched. The confirmation run results were then incorporated to refine the initial working model.

### 3.4.2 Specimens, Environment, and Loading

Cadmium-plated 4340 steel samples heat treated to 5 different material strengths, as previously described, were tested in accordance with ASTM-F519. The specimen material demonstrated adequate hydrogen sensitivity. The cadmium-plated specimens used for these experiments are depicted in Fig. 15. The 1d specimens were directly loaded with nut and bolt. The loads were monitored via loading rings installed in the load path. The load rings were calibrated prior to the experiments. For this phase, loads were applied as a percentage (45%–95%) of the calculated 100% NFS determined for each geometry. Ten specimens were used to calculate the average 100% NFS with the identical fixturing applied during the experiments. Ten specimens from each group were loaded to failure. The experimental loading was then applied as a percentage of this determined average NFS failure load. Loads were recorded with data sampling hardware and software for the other geometries. Figures 16A–D depict the in situ test apparatus for the experiments.

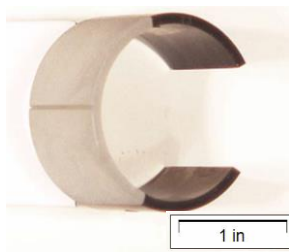


**Fig. 15 Cadmium-plated experimental specimens, type 1d**

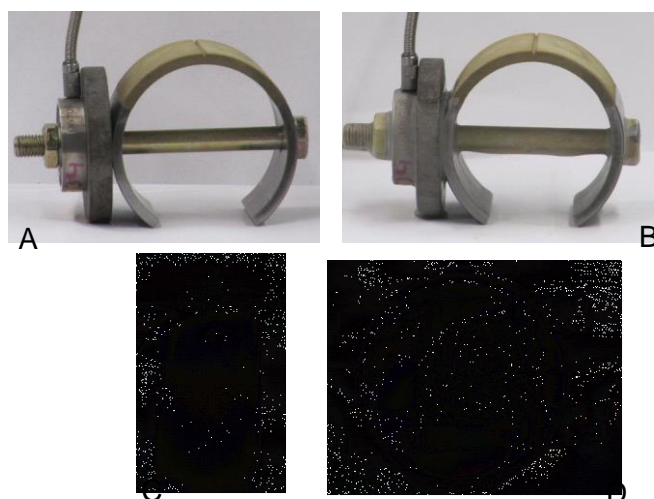


**Fig. 16 Phase 2 geometry 1d in situ environmental setup: A) loaded, B) loaded and masked, C) being tested in solution, and D) top-down perspective**

The specimens were masked so that only the plated surface contacted the test solution. The solution used was diluted with deionized water in 5 different concentrations: 2, 3.4, 17.3, 30, and 34.5 vol% in accordance with Table 6. The loaded specimens were then immersed in solution for the duration of the experiment. Specimens were removed upon failure or after sustained load of 168 h.

The life models were then used in the confirmation test portion of the matrix to choose appropriate parameters to both enhance and verify the model. Final life prediction equations and 3-D models were created after the incorporation of the confirmation data.

### **3.5 Results**

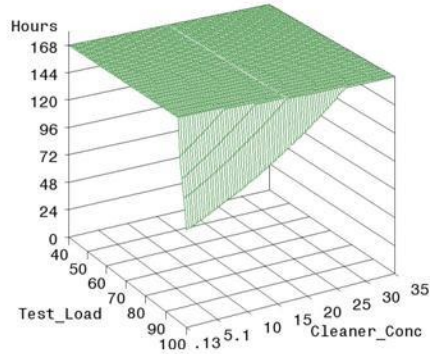
Figs. 17–21 show the final graphical life prediction model for each chemical. The final life prediction models for each respective geometry and material did not vary significantly from the preliminary set, thus verifying the initial prediction. The variables in the models are material strength, test load, and chemical concentration. The models yield time-to-failure predictions.

# Results

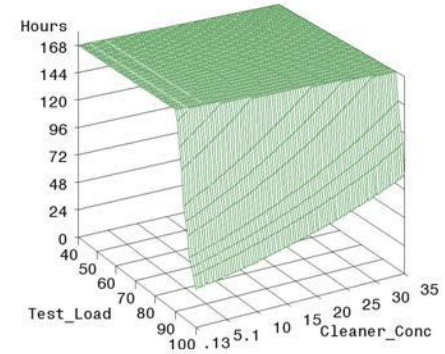
## Brulin 815GD



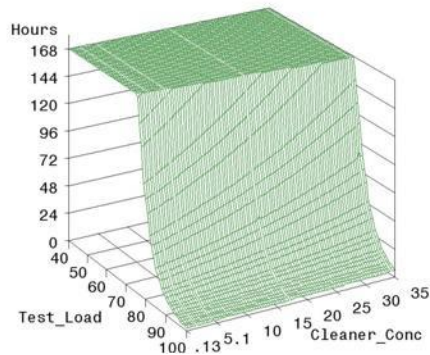
Predicted Median Lifetime  
Strength=T1 (210 KSI)



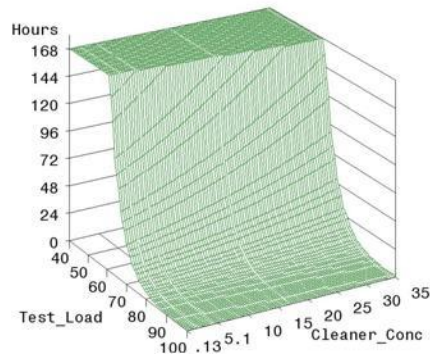
Predicted Median Lifetime  
Strength=T2 (220 KSI)



Predicted Median Lifetime  
Strength=T3 (245 KSI)



Predicted Median Lifetime  
Strength=T4 (270 KSI)



Predicted Median Lifetime  
Strength=T5 (280 KSI)

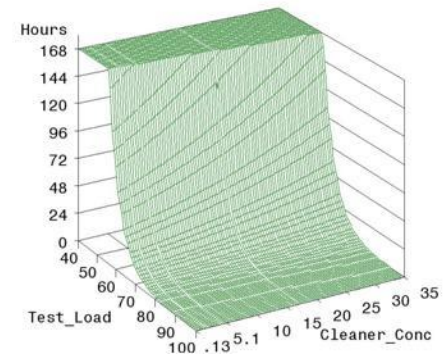


**Fig. 17 Final Brulin 815 GD life prediction models**

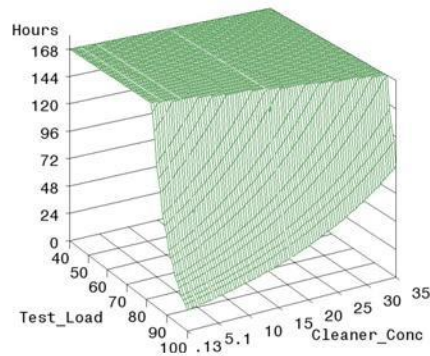


# Results

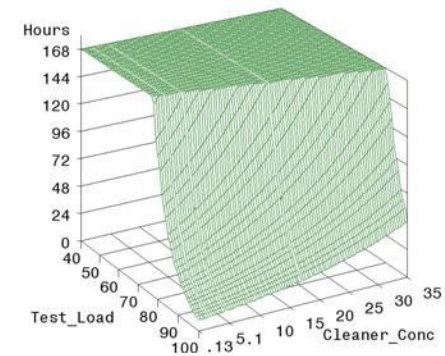
Brulin 1990GD



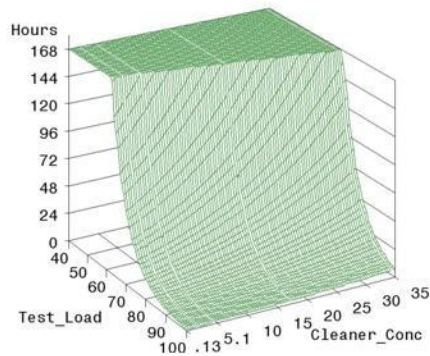
Predicted Median Lifetime  
Strength=T1 (210 KSI)



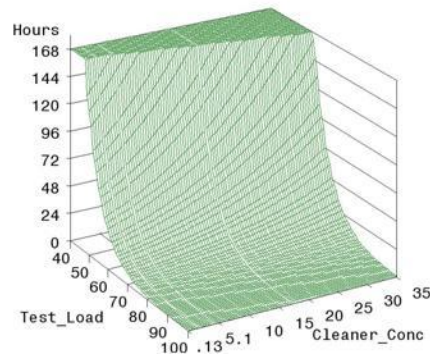
Predicted Median Lifetime  
Strength=T2 (220 KSI)



Predicted Median Lifetime  
Strength=T3 (245 KSI)



Predicted Median Lifetime  
Strength=T4 (270 KSI)



Predicted Median Lifetime  
Strength=T5 (280 KSI)

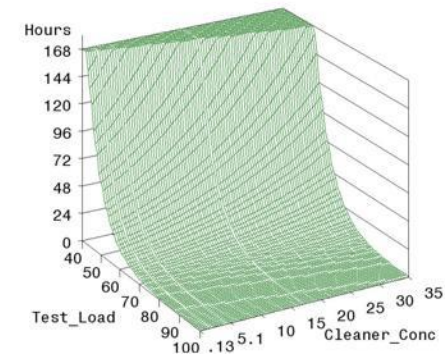


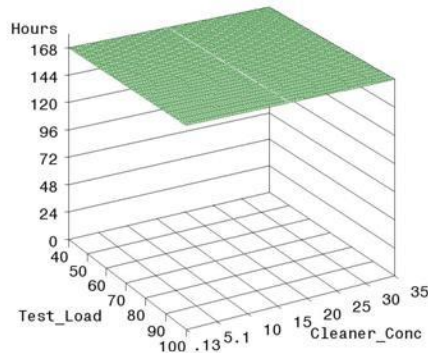
Fig. 18 Final Brulin 1990 GD life prediction models

# Results

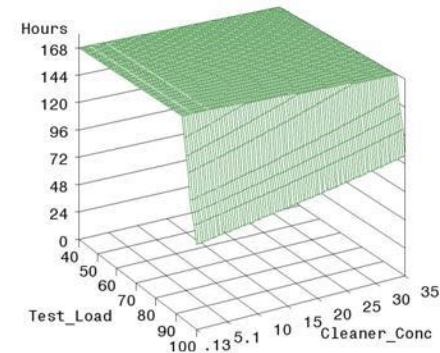
Cee Bee 300LFM



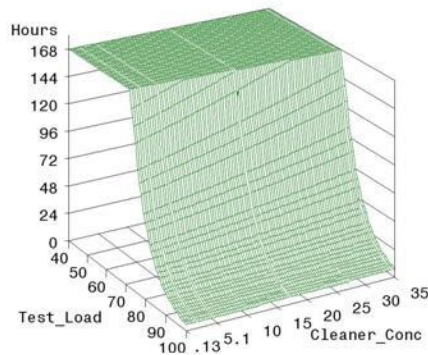
Predicted Median Lifetime  
Strength=T1 (210 KSI)



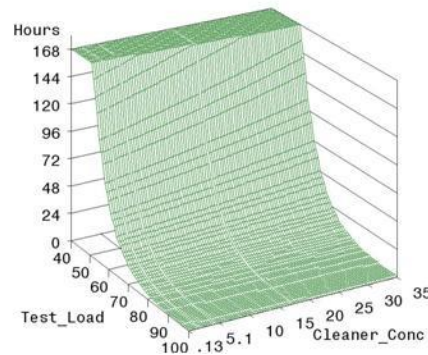
Predicted Median Lifetime  
Strength=T2 (220 KSI)



Predicted Median Lifetime  
Strength=T3 (245 KSI)



Predicted Median Lifetime  
Strength=T4 (270 KSI)



Predicted Median Lifetime  
Strength=T5 (280 KSI)

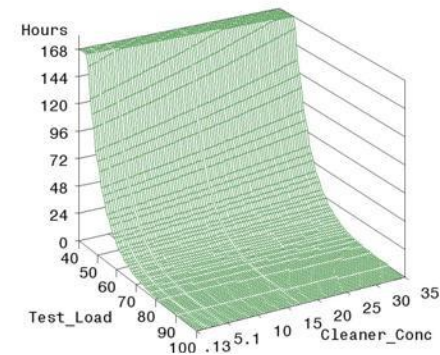


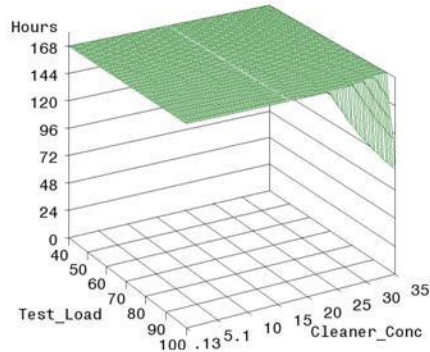
Fig. 19 Final Cee Bee 300 LFM life prediction models

# Results

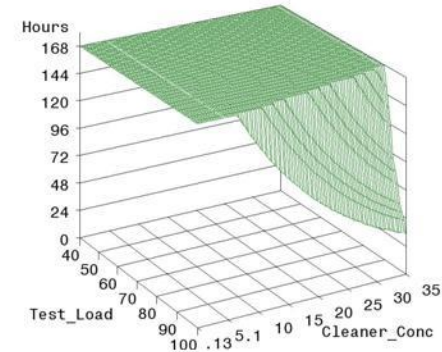
Calla 602 LF



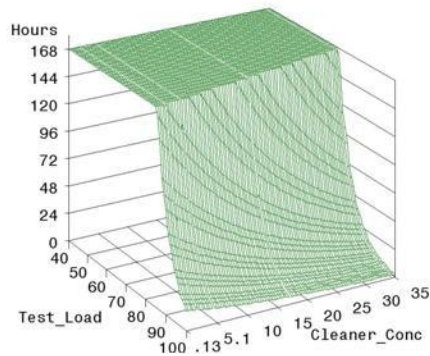
Predicted Median Lifetime  
Strength=T1 (210 KSI)



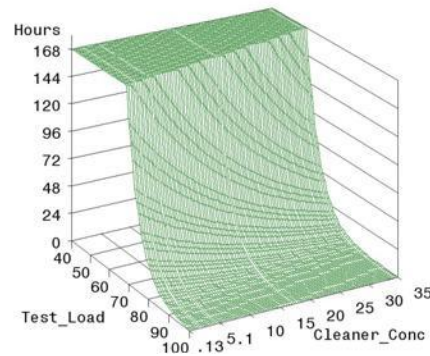
Predicted Median Lifetime  
Strength=T2 (220 KSI)



Predicted Median Lifetime  
Strength=T3 (245 KSI)



Predicted Median Lifetime  
Strength=T4 (270 KSI)



Predicted Median Lifetime  
Strength=T5 (280 KSI)

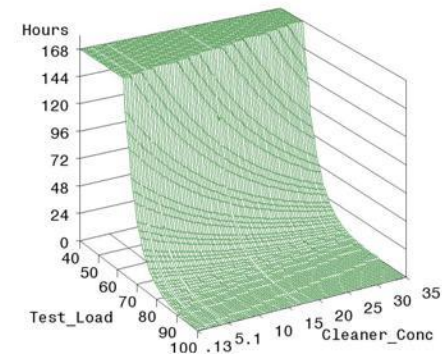


Fig. 20 Final Calla 602 LF life prediction models

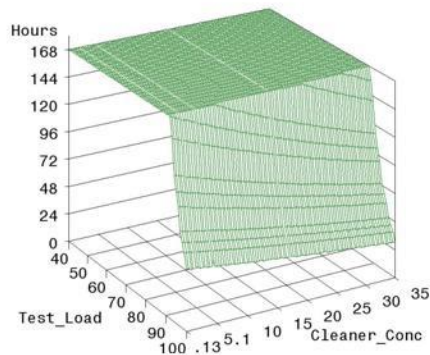


# Results

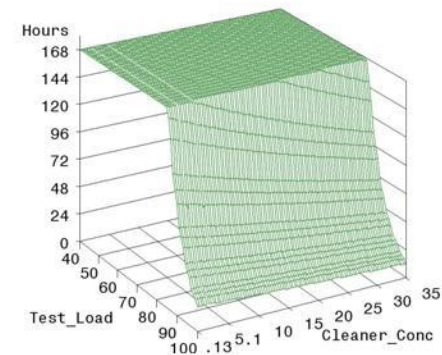
## Daraclean 282



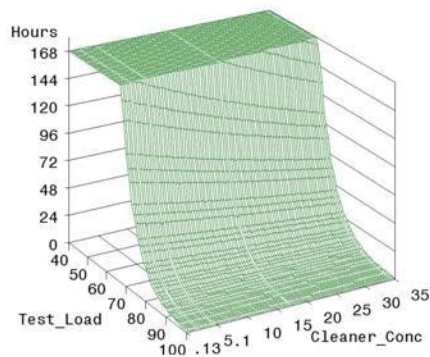
Predicted Median Lifetime  
Strength=T1 (210 KSI)



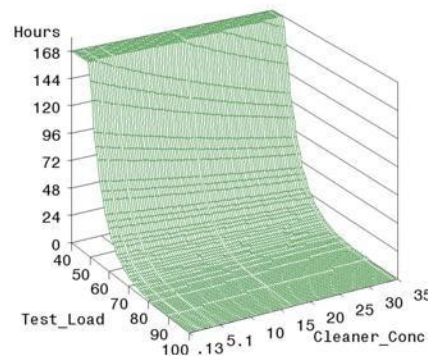
Predicted Median Lifetime  
Strength=T2 (220 KSI)



Predicted Median Lifetime  
Strength=T3 (245 KSI)



Predicted Median Lifetime  
Strength=T4 (270 KSI)



Predicted Median Lifetime  
Strength=T5 (280 KSI)

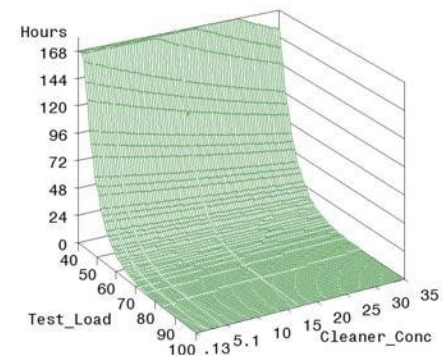


Fig. 21 Final Daraclean 282 life prediction models

### 3.6 Discussion

---

The results were extremely rewarding in that they clearly demonstrate differences among the test chemicals. The predictive models express hydrogen sensitivity in terms of applied load, material strength, and hydrogen environment. In this case, the hydrogen environment is the maintenance cleaning solution. The time duration, 168 h, is above that which is accepted as the representative lifetime cutoff for service environments, 150 h. Essentially, these data suggest that if the material demonstrates no hydrogen sensitivity in the test environment for 168 h at a specific strength and applied load combination, then it should not be expected to fail in a lifetime of service maintenance at that strength and applied load level. The safe zone in the graphical representation of the models is the area below the curves.

A comparison with all models across test chemicals shows that nearly all the chemicals do not produce a severe enough environment to induce hydrogen re-embrittlement at or below the 210-ksi strength level. In fact, they are all tolerant of an applied load of approximately 75% of their NFS at 220 ksi. This does not mean that in an environment that emits more hydrogen, no sensitivity would be expected.

Although varying performance can be observed across test chemicals, the trends are in agreement. The sensitivity increases with material strength level, applied load, and to a lesser degree, with cleaner concentration. All of these trends are in line with traditional expectations. While material strength level is typically given consideration with regard to hydrogen sensitivity, applied load is often forgotten. Residual stresses from forming, quenching, or assembly can often reach 35%–40% of the UTS. This is important to remember since these life prediction models show sensitivity beginning at, or even below, that region. This supports traditional findings where components sometimes break on the shelf while waiting to be placed in service. When combined with a design stress or in-service applied stress, catastrophic failure is much more likely to occur. The degree of heightened sensitivity from applied stress was unknown before now, since it has never been investigated.

It can also be observed in the data that the Daraclean 282 and Brulin 1990 GD show the harshest environment. The coupons were significantly affected even down at the 245-ksi material strength level. The Calla 602 LF appeared the mildest with the coupons showing no effect until 245 ksi. The Cee Bee 300 cleaner showed promise and is likely that it would have performed better on the upper end of the material strength with the addition of more corrosion inhibitor in

the cleaner. The hydrogen sensitivity observed with these maintenance chemicals is largely reflective of the additive corrosion inhibitor's ability to reduce corrosion. Corrosion of the material contributes significantly to the amount of hydrogen absorbed. It is not the sole source, however, as all non-neutral solutions have free hydrogen ions that may be absorbed by metals upon contact.

The 2 Brulin products and the Cee Bee chemical show a positive slope with concentration, while the Calla and Daraclean demonstrate a negative slope. These 2 products perform better at lower concentrations.

### **3.7 Conclusions**

---

The following conclusions can be drawn from the data developed and discussion of this phase.

- Life prediction models were developed that accurately represent the expected hydrogen sensitivity for the maintenance chemicals over the range of parameters explored for VAR 4340 steel.
- The trends observed in the data were consistent across all chemicals tested. Sensitivity increases with applied load and material strength. Results with respect to cleaner concentration were mixed.
- Applied stress has the most direct effect on hydrogen sensitivity, while material strength is a close second. Increasing the value of either parameter directly heightens the sensitivity to hydrogen, as one might expect.
- High residual stress levels (35%–40% of UTS) alone are capable of inducing hydrogen embrittlement without further applied system stresses as long as the material strength above 270 ksi is great enough.
- Based on the specific test conditions used for this study, the Daraclean 282 appears to be the harshest of the chemicals tested.

## **4. Phase 3**

---

---

### **4.1 Introduction**

---

In this phase, 4 prospective cadmium alternative coatings (ion vapor deposition [IVD] aluminum, Alumiplate, Dipsol Zn-Ni, Atotech Zn-Ni) and cadmium were tested in an aqueous cleaner to mimic the industrial maintenance cycle. The DoE approach was used to vary parameters over a range of material strength, load

level, and maintenance cleaning solution concentration, for aerospace grade (SAE-AMS-6414) 4340 steel. The ASTM-F519 type 1d geometry was employed while monitoring load to determine the precise time to fracture for the specific set of parameters. This allowed comparisons across coating, material strength, and test solution concentration to be drawn. Incorporating the failure time, load, and stress levels into failure models yielded predictive equations over broad parameter ranges. Reliable predictions of hydrogen sensitivity under specific conditions were then realized for each coating.

## **4.2 Objective**

---

This phase was designed to use a DoE approach to create life prediction models for VAR steel, SAE-AMS-6414.<sup>2</sup> The ASTM-F519 Type 1d specimen geometry in combination with load cell measurement and time monitored experiments were employed.<sup>1</sup> This phase evaluated the most prospective environmentally friendly cadmium alternative coatings that currently have their use limited via the perceived risk of hydrogen embrittlement. Demonstrating that these alternative coatings have safe zones below threshold material strengths and load levels provide the rationale to relax the current risk assessment baking requirements to further implement prospective cadmium alternatives on aerospace materials. This should also greatly increase the applications for which the replacements will be considered, as the models provide the acceptability criteria for the relevant parameters specific to each application.

## **4.3 Materials**

---

The type 1d c-ring specimen geometry used in this phase was fabricated from SAE-AMS-6414 VAR steel and was manufactured in accordance with ASTM-F519. These specimens were used in the previous phases to investigate the effects of steel cleanliness and maintenance chemicals on hydrogen susceptibility. The specimen is depicted in Fig. 13.

### **4.3.1 Heat Treating**

As in the other phases, it was crucial to have the strength level of each specimen in a very narrow range ( $\pm 5$  ksi); otherwise, data variation based on geometry might not be observable in the output. The team constructed a submatrix for the background work. This process entailed certification of a rack-basket, hardening furnace, and tempering furnace by normalizing, hardening, and tempering samples to 280 ksi using small cylindrical buttons for in-process hardness tests and verification tensile samples. Once tested, verified, and certified per mutually agreed parameters, furnaces and ovens had the process frozen for approval. The

heat treatments of the actual specimens were completed within 30 days of the date of frozen planning approval. There were 5 heat treatment batches for this work. Each batch of specimens, T1–T5, required heat treatment in accordance with the following:

- T1 =  $140 \pm 5$  ksi (135–145 ksi)
- T2 =  $158 \pm 5$  ksi (153–163 ksi)
- T3 =  $210 \pm 5$  ksi (205–215 ksi)
- T4 =  $262 \pm 5$  ksi (257–267 ksi)
- T5 =  $280 \pm 5$  ksi (275–285 ksi)

The specimen counts varied by temper level following the overall DoEs. The individual quantities were derived from the DoE matrix further explained in the Phase 3 experimental procedures section (Section 4.4).

- T1 = 30 + 6 tensiles
- T2 = 75 + 6 tensiles
- T3 = 180 + 6 tensiles
- T4 = 75 + 6 tensiles
- T5 = 45 + 6 tensiles

#### 4.3.2 Coatings

There were 4 coatings selected for this phase. The most prospective cadmium alternatives were selected, and cadmium served as a control group for comparison.

- 1) **Dipsol Zn-Ni:** Cyanide free, electroplated alkaline LHE Zn-Ni. The coating was plated to USAF Drawing No. 201027456, Class 1 (0.5 to 0.8 mil), Type II (with supplementary Dipsol IZ-264 trichrome conversion coat applied prior to bake).<sup>5</sup>
- 2) **Atotech Zn-Ni:** Cyanide free, electroplated alkaline LHE Zn-Ni. The coating was plated to BAC 5680 Class 1 (0.5 to 0.8 mil), Type II (with supplementary Dipsol IZ-264 trichrome conversion coat applied prior to bake).<sup>6</sup>



- 3) **Alumiplate:** Solvent-based electroplating. The coating was plated to MIL-DTL-83488D, Class 2 (0.5 to 0.8 mil), Type II (with supplementary trivalent chromate conversion coat per MIL-DTL-5541 Type II, Class 1A).<sup>7,8</sup>
- 4) **IVD aluminum:** Ion vapor deposition. The coating was applied in accordance with MIL-DTL-83488D, Class 1 (1.0 to 1.3 mil), Type II (with supplementary chromate conversion coat per MIL-DTL-5541 Type I, Class 1A) and McDonnell Douglas PS13143.<sup>7,8</sup>
- 5) **Cadmium:** The cadmium plating was LHE cadmium in accordance with MIL-STD-870 Rev. C. Type II, Class 1.<sup>4</sup>

The plating requirements were critical since the surface area plated affects both the amount of hydrogen introduced into the sample and the free path out of the sample during hydrogen bake relief. Specimens were supplied in the stress-relieved condition to an aerospace industry approved plating/coating vendor. The ends were masked, specimens were plated/coated, and then postprocess baked at  $375 \pm 25$  °F within 1 h of plating (except for IVD aluminum and Alumiplate specimens, these were not baked). The masking requirements were set such that no fluid would contact bare unplated steel during re-embrittlement testing. The plated area of the specimens was in accordance with the Fig. 14.

#### **4.3.3 Immersion Chemical**

Daraclean 282 proved to be the most embrittling commonly used maintenance aqueous cleaner among the 5 evaluated in Phase 2. It is an approved aerospace cleaner at many DoD and industrial facilities. Therefore, Daraclean 282 was selected for this matrix in an attempt to encapsulate the worst-case scenario in terms of embrittling potential. The fluid was maintained at 180 °F, and the chemical concentration ranged from 2 to 35 vol%.

### **4.4 Experimental Procedures**

---

#### **4.4.1 Design of Experiment**

This approach was used over a range of material strength, load level, and hydrogen environment. The specimens were tested while load levels were monitored to determine a precise time to fracture at specific percentages of NFS, specific material strengths (heat treat tempers T1–T5), and specific hydrogen-emitting environment (Daraclean 282 vol%). Contrary to the existing standard,

greater information was gleaned beyond the result of a pass/fail test. Once the failure time, load, and stress level data were incorporated into DoE failure models, predictive equations over the broad ranges were developed.

The DoE focused on 3 variables. The control variables were selected from risk reduction and ruggedness leveraged efforts conducted by The Boeing Company with the assistance of ARL. Table 10 presents the range of test conditions for the test geometry researched.

**Table 10 Phase 3 design of experiment conditions matrix**

<b>Condition</b>	<b><math>-\alpha</math></b>	<b><math>-</math></b>	<b><math>0</math></b>	<b><math>+</math></b>	<b><math>+\alpha</math></b>
Strength (ksi)	140	158	210	262	280
Test load (% NFS)	35	45	60	75	95
Daraclean 282 vol%	2	4.5	17.3	30	34.5

Below 140 ksi steel is generally accepted as not being sensitive to hydrogen, which set the lower limit for strength. Daraclean was not used at concentrations near 0%, essentially completely deionized water, since the working group had experience that deionized water is actually severely corrosive and a very harsh environment for steel. It is also not a real-world environment.

The DoE approach was refined with preliminary ruggedness and risk reduction efforts at Boeing-Mesa, with technical assistance from Boeing-St. Louis, Boeing-Seattle, and ARL. Typical of DoEs, it consisted of 3 test portions, a linear portion, a quadratic portion, and a confirmation portion. The example matrix presented in Tables 11–13 with the condition values corresponding to Table 10. These experiments aided the development of appropriate boundary conditions for the larger effort.

**Table 11 Phase 3 linear portion test matrix**

Repeat Entire Matrix 2×	Run ID	A	B	C	Run Order
		Strength (ksi)	Test Load (% NFS)	Daraclean (wt%)	
Linear portion	L1	–	–	–	Random
	L2	–	–	+	
	L3	–	+	–	
	L4	–	+	+	
	L5	+	–	–	
	L6	+	–	+	
	L7	+	+	–	
	L8	+	+	+	
Center points	C1	0	0	0	
	C2	0	0	0	
	C3	0	0	0	
	C4	0	0	0	
	C5	0	0	0	
	C6	0	0	0	

**Table 12 Phase 3 quadratic portion test matrix**

Repeat Q1–Q6 5×	Run ID	A	B	C	Run Order
		Strength (ksi)	Test Load (% NFS)	Daraclean (wt%)	
Not replicated	C7	0	0	0	First
Quadratic portion	Q1	$+\alpha$	0	0	Random
	Q2	$-\alpha$	0	0	
	Q3	0	$+\alpha$	0	
	Q4	0	$-\alpha$	0	
	Q5	0	0	$+\alpha$	
	Q6	0	0	$-\alpha$	
Not replicated	C8	0	0	0	Last

**Table 13 Phase 3 confirmation portion test matrix**

	Run ID	A	B	C	Run Order
		Strength (ksi)	Test Load (% NFS)	Daraclean (wt%)	
Confirmation portion	1				
	2				
	3				
	4				
	5				
	6				
	7				
	8	Varied depending on outcome of linear, center, and quadratic			Random
	9				
	10				
	11				
	12				
	13				
	14				
	15				
	16				

After the linear and center point data runs were completed, initial calculations were made for the predictive model equations. Those initial models were utilized to choose confirmation runs to be researched. The confirmation run results were then incorporated to refine the initial working model.

#### 4.2.2 Specimens, Environment, and Loading

The 4340 steel samples heat treated to 5 different material strengths, as previously described, were tested in accordance with ASTM-F519. The specimen material demonstrated adequate hydrogen sensitivity. The cadmium-plated specimens used for these experiments are depicted in Fig. 15. The other coatings were similarly plated. The 1d specimens were directly loaded with nut and bolt. The loads were monitored via loading rings installed in the load path. The load rings were calibrated prior to the experiments. For this phase, loads were applied as a percentage (35%–95%) of the calculated 100% NFS determined for each geometry. Ten specimens were used to calculate the average 100% NFS with the identical fixturing applied during the experiments. Ten specimens from each group were loaded to failure. The experimental loading was then applied as a percentage of this determined average NFS failure load. Loads were recorded with data sampling hardware and software for the other geometries. Figures 16A–D depict the in situ test apparatus for the experiments.

The specimens were masked so that only the plated surface contacted the test solution. The solution used was diluted with deionized water in 5 different concentrations: 2, 3.4, 17.3, 30, and 34.5 vol% in accordance with Table 10. The loaded specimens were then immersed in solution for the duration of the experiment. Specimens were removed upon failure or after sustained load of 168 h.

The life models were then used in the confirmation test portion of the matrix to choose appropriate parameters to both enhance and verify the model. Final life prediction equations and 3-D models were created after the incorporation of the confirmation data.

## **4.5 Results**

---

Figures 22–26 show the final graphical life prediction model for each coating. The final life prediction models for each respective geometry and material did not vary significantly from the preliminary set, thus verifying the initial prediction. The variables in the models are material strength, test load, and Daraclean 282 concentration. The models yield time-to-failure predictions

.

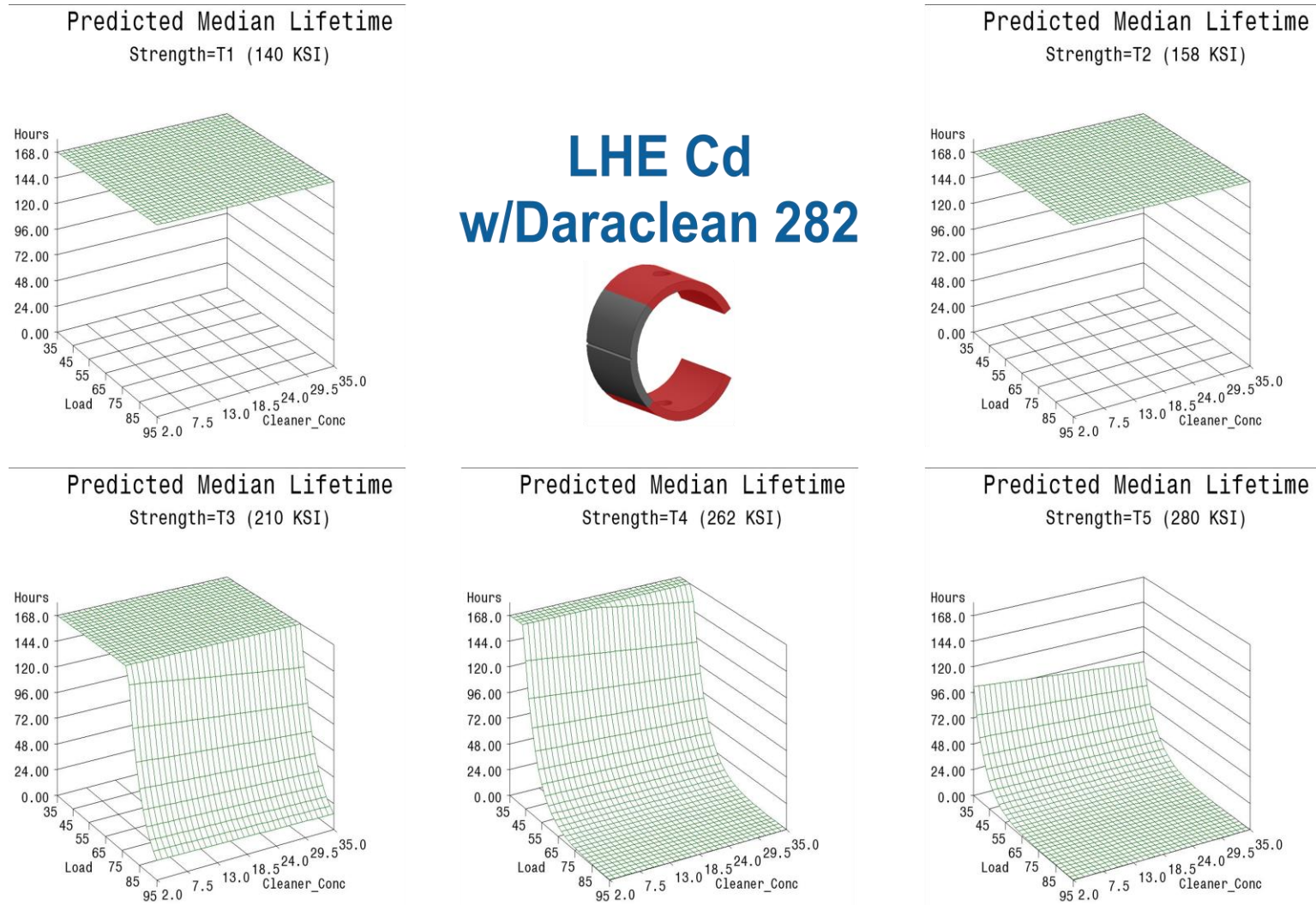


**Fig. 22 Final LHE cadmium with Daraclean 282 life prediction models**

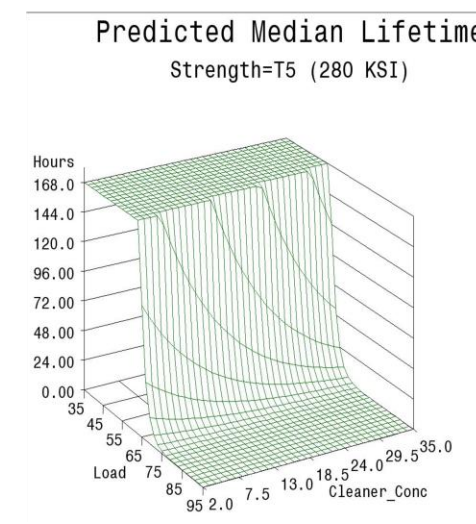
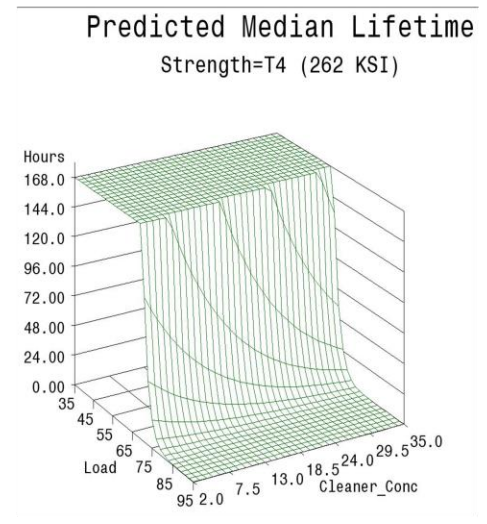
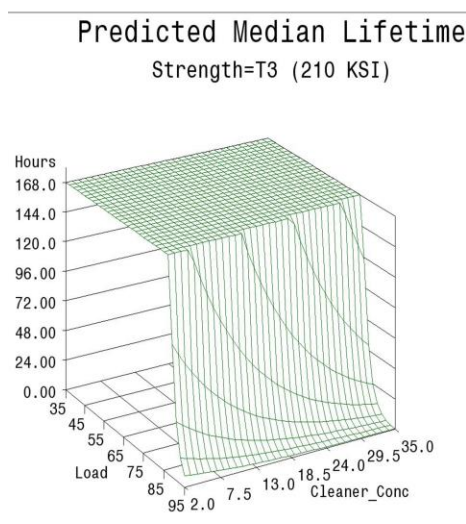
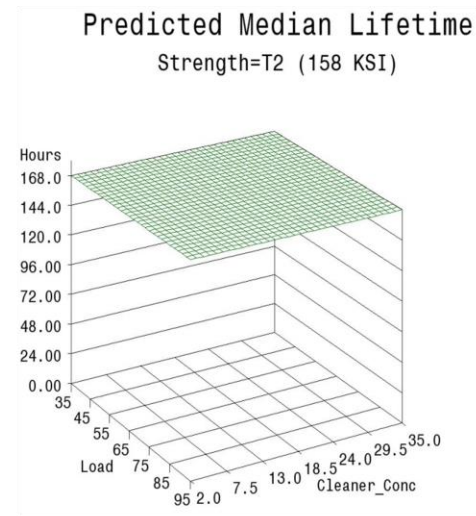
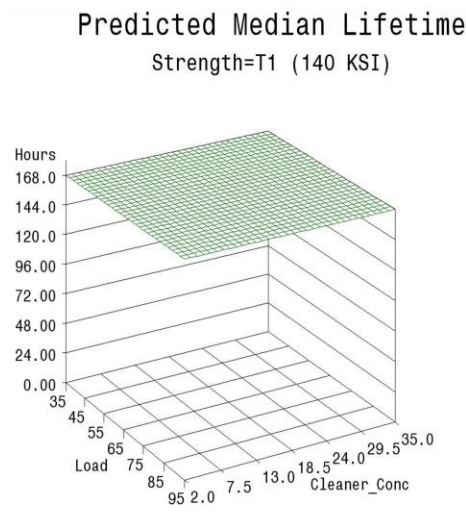


**Fig. 23 Final Alumiplate with Daraclean 282 life prediction models**



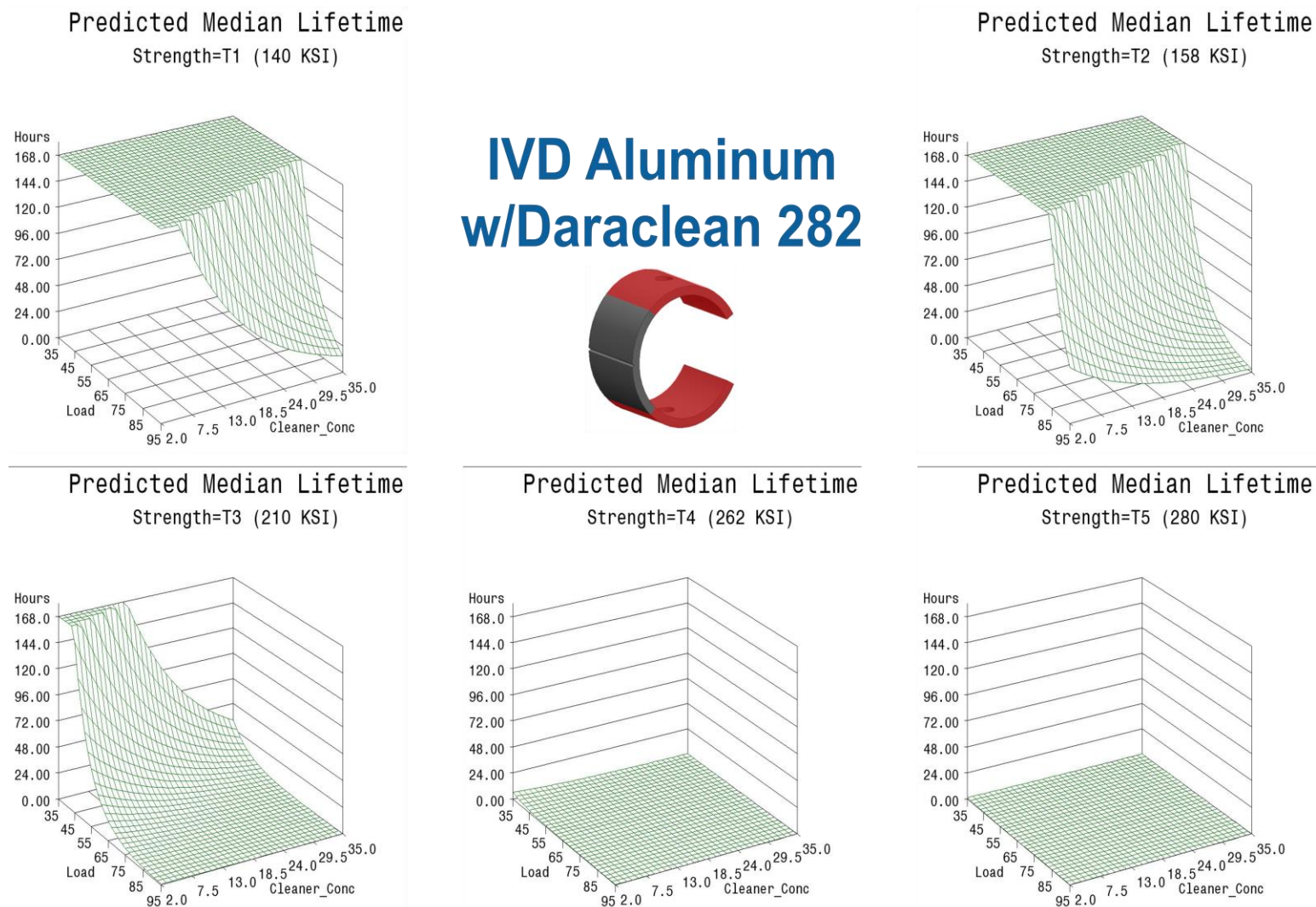


**Fig. 24 Final IVD aluminum with Daraclean 282 life prediction models**



# Atotech Alkaline LHE Zn-Ni w/Daraclean 282

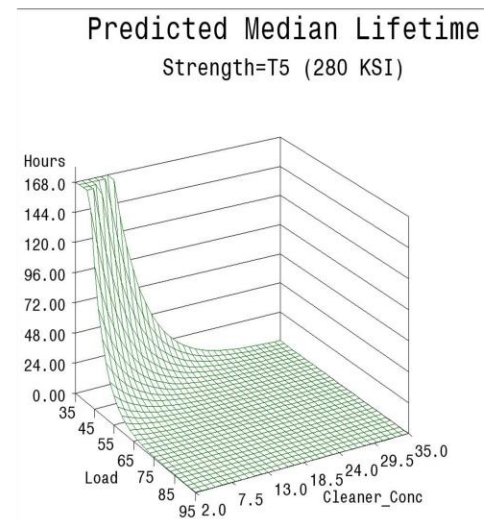
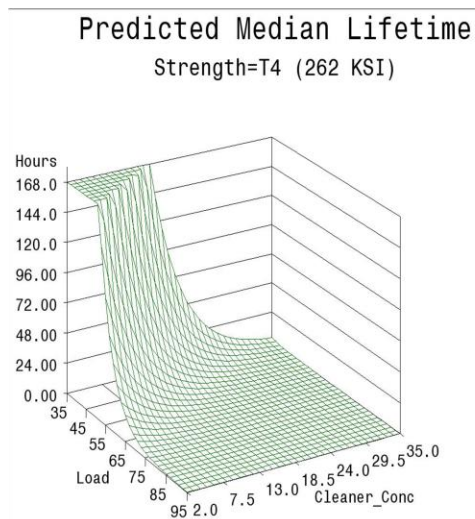
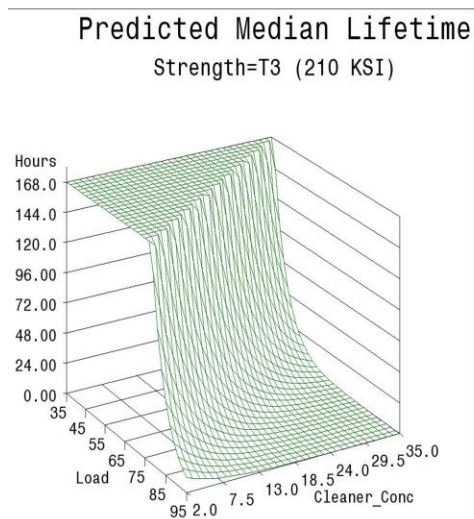
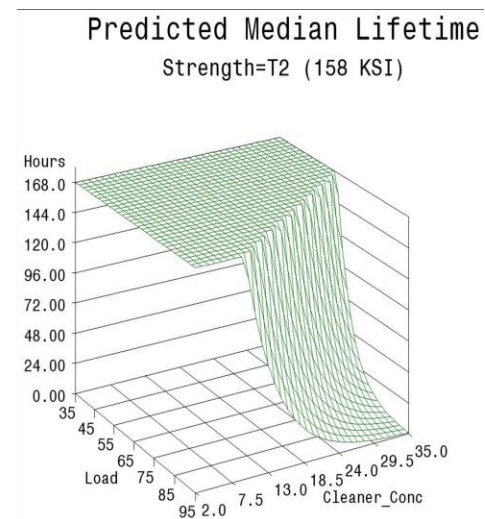
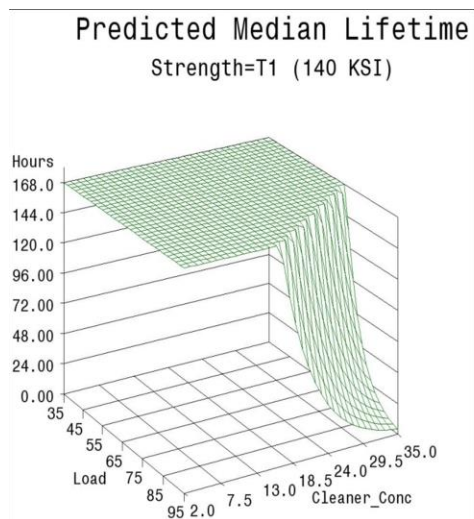


**Fig. 25 Final Atotech Alkaline LHE Zn-Ni with Daraclean 282 life prediction models**

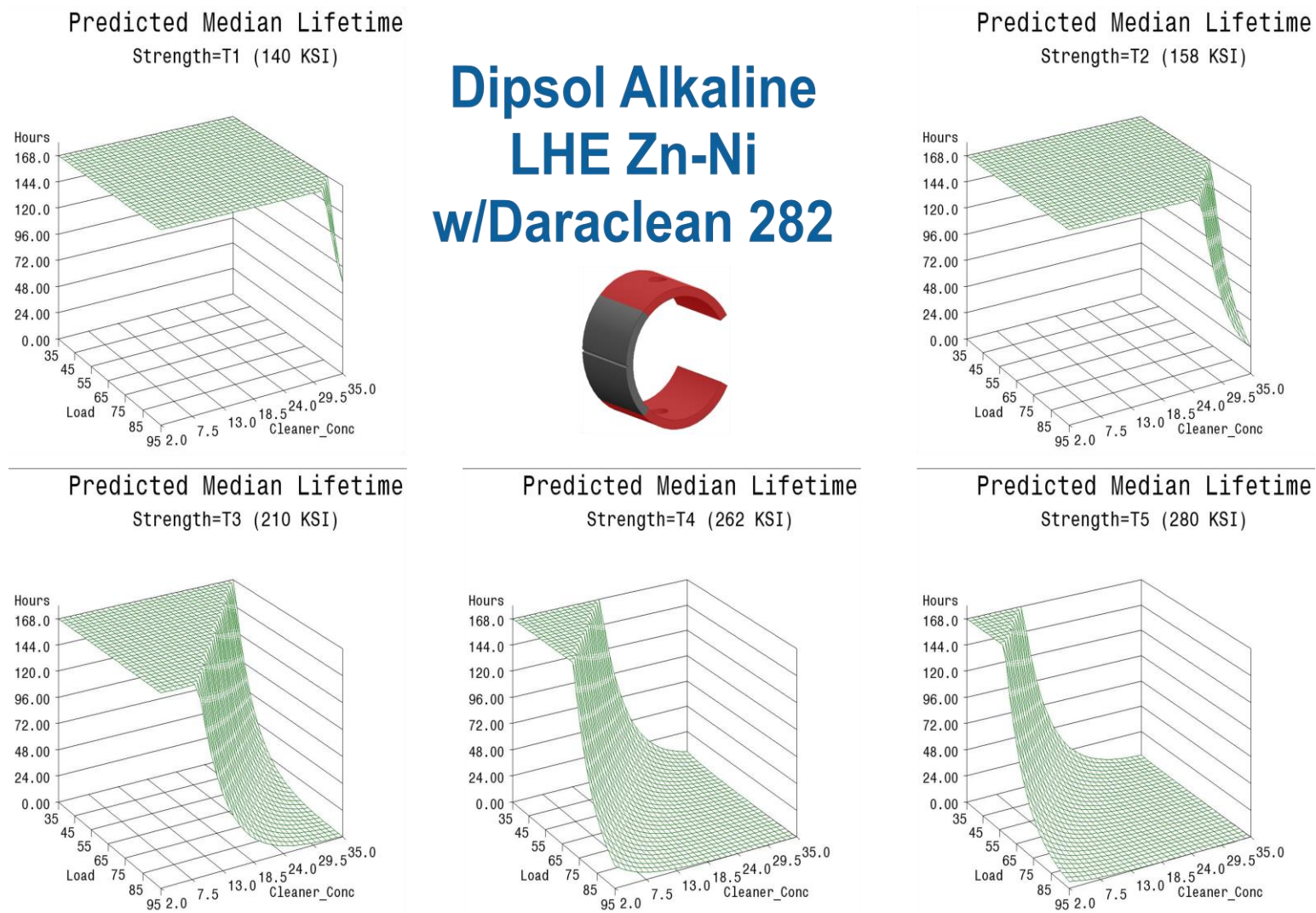


**Fig. 26 Final Dipsol Alkaline LHE Zn-Ni with Daraclean 282 life prediction models**

## 4.6 Discussion

---

The results were extremely rewarding in that they clearly demonstrate differences among the test coatings. The predictive models express hydrogen sensitivity in terms of applied load, material strength, and hydrogen environment. In this case, the hydrogen environment is the Daraclean 282 maintenance cleaning solution. The time duration, 168 h, is above that which is accepted as the representative lifetime cutoff for service environments, 150 h. Essentially, these data suggest that if the material demonstrates no hydrogen sensitivity in the test environment for 168 h at a specific strength and applied load combination, then it should not be expected to fail in a lifetime of service maintenance at that strength and applied load level. The safe zone in the graphical representation of the models is the area below the curves.

A comparison with all of the models across test coating shows that the LHE cadmium and Alumiplate coatings in combination with the test solution do not produce a severe enough environment to induce hydrogen embrittlement at or below the 158-ksi strength level when the cleaner concentration is at or below 35 vol%. The “T1, 140 ksi” and “T2, 158 ksi” graphs for these 2 coatings are flat, showing no sensitivity, whereas the Dipsol LHE Zn-Ni coating shows no sensitivity to hydrogen embrittlement at or below 158 ksi only when the cleaner concentration is at or below 25 vol%. The “T1, 140 ksi” and “T2, 158 ksi” graphs for this coating are predominantly flat, except for a small corner where the cleaner concentration and load are very high. However, for all of these coatings, this does not mean that in an environment that emits more hydrogen, no sensitivity would be expected.

Although varying performance can be observed across test coating, the trends are in agreement. The sensitivity increases with material strength level, applied load, and to a lesser degree, with cleaner concentration. All of these trends are in line with traditional expectations. While material strength level is typically given consideration with regard to hydrogen sensitivity, applied load is often forgotten. Residual stresses from forming, quenching, or assembly can often reach 35%–40% of the UTS. This is important to remember since these life prediction models show sensitivity beginning at or even below that region. This supports traditional findings where components sometimes break on the shelf while waiting to be placed in service. When combined with a design stress or in-service applied stress, catastrophic failure is much more likely to occur. The degree of heightened sensitivity from applied stress was unknown before now, since it has never been investigated.

It can also be observed in the data that the IVD aluminum shows the greatest sensitivity. It was significantly affected even down at the 140 ksi material strength level. The Alumiplate was the least affected showing no effect until 210 ksi. While the others are somewhat porous coatings, Alumiplate is a good barrier coating. The 2 Zn-Ni coatings performed similarly, but the Dipsol process was deemed better. Both performed on par with cadmium, but not quite as well as Alumiplate.

These test coatings and environment combinations may not be representative of every application. One would be able to apply a factor of safety to these life prediction models and have confidence that similar applications would not fail due to hydrogen embrittlement. All the models have similar trends, but a risk analysis would likely scale from a worst case and not middle of the pack performance.

## **4.7 Conclusions**

---

The following conclusions can be drawn from the data developed and discussion of this phase.

- Life prediction models were developed that accurately represent the expected hydrogen sensitivity for the coatings in Daraclean 282 over the range of parameters explored for VAR 4340 steel.
- The trends observed in the data were reasonably consistent across all coatings. Sensitivity increases with applied load, material strength, and to a lesser degree cleaner concentration.
- Applied stress has the most direct effect on hydrogen sensitivity, while material strength is a close second. Increasing the value of either parameter directly heightens the sensitivity to hydrogen, as one might expect.
- High residual stress levels (35%–40% of UTS) alone are capable of inducing hydrogen embrittlement without further applied system stresses as long as the material strength and cleaner concentration are great enough.
- The cadmium baseline demonstrated minimal hydrogen sensitivity below the 200-ksi material strength level.
- IVD aluminum demonstrated the highest sensitivity to hydrogen, being significantly affected even at 140-ksi material strength.

- The Dipsol and Atotech Zn-Ni processes showed strong dependence on chemical concentration.
- Based on the specific test conditions used for this study, the Dipsol Zn-Ni process appears safe for strength below 210 ksi, as long as the chemical concentration is kept low, below 10%.

## 5. References

---

1. ASTM-F519-13. Standard test method for mechanical hydrogen embrittlement evaluation of plating/coating processes and service environments. West Conshohocken (PA): ASTM International; 2013.
2. SAE-AMS-6414K-2007. Steel, bars, forgings, and tubing 0.80Cr - 1.8Ni - 0.25Mo (0.38 - 0.43C) (SAE 4340) vacuum consumable electrode remelted. Warrendale (PA): SAE World Headquarters; 2007.
3. SAE-AMS-6415S-2007. Steel, bars, forgings, and tubing 0.80Cr - 1.8Ni - 0.25Mo (0.38 - 0.43C). (SAE 4340). Warrendale (PA): SAE World Headquarters; 2007.
4. MIL-STD-870C. Department of Defense standard practice: cadmium plating, low embrittlement, electro-deposition. Hill Air Force Base, (UT): Ogden Air Logistics Center; 2009 Apr 27.
5. US Air Force. Drawing No. 201027456. Hill Air Force Base (UT): US Air Force; 2010.
6. BAC 5680. LHE Zn-Ni plating specification. Chicago (IL): The Boeing Company, 2008.
7. MIL-DTL-83488D. Coating, aluminum, high purity. Wright-Patterson AFB (OH): Air Force Life Cycle Management Center; 1999 Apr 1.
8. MIL-DTL-5541F. Chemical conversion coatings on aluminum and aluminum alloys. Lakehurst (NJ): Naval Air Warfare Center Aircraft Division; 2006 Jul 11.

## List of Symbols, Abbreviations, and Acronyms

---

AMS	Aerospace Material Specification
ARL	US Army Research Laboratory
ASTM	American Society for Testing and Materials
DOD	Department of Defense
DoE	design of experiment
ESTCP	Environmental Security Technology Certification Program
IVD	ion vapor deposition
LHE	low hydrogen embrittlement
NFS	notch fracture strength
OEM	original equipment manufacturer
SAE	Society of Automotive Engineers
SERDP	Strategic Environmental Research and Development Program
UTS	ultimate tensile strength
VAR	vacuum-arc-remelted
Zn-Ni	zinc-nickel

1 DEFENSE TECHNICAL  
(PDF) INFORMATION CTR  
DTIC OCA

2 DIRECTOR  
(PDF) US ARMY RESEARCH LAB  
RDRL CIO LL  
IMAL HRA MAIL & RECORDS  
MGMT

1 GOVT PRINTG OFC  
(PDF) A MALHOTRA

1 DIR USARL  
(PDF) RDRL WMM F  
S GREND AHL